Monthly Notices of the ROYAL ASTRONOMICAL SOCIETY

MNRAS **499,** 3630–3649 (2020) doi:10.1093/mnras/staa3064
Advance Access publication 2020 October 6

A pair of Jovian Trojans at the L4 Lagrange point

Timothy R. Holt [1,2]★ David Vokrouhlický,[3] David Nesvorný,[2] Miroslav Brož[3] and Jonathan Horner[1]

[1]*Centre for Astrophysics, University of Southern Queensland, Toowoomba, Queensland 4350, Australia*
[2]*Southwest Research Institute, Department of Space Studies, 1050 Walnut St., Ste 300, Boulder, CO-80302, USA*
[3]*Institute of Astronomy, Charles University, V Holešovičkách 2, Prague 8 CZ-180 00, Czech Republic*

Accepted 2020 September 24. Received 2020 September 14; in original form 2020 August 3

ABSTRACT

Asteroid pairs, two objects that are not gravitationally bound to one another, but share a common origin, have been discovered in the Main belt and Hungaria populations. Such pairs are of major interest, as the study of their evolution under a variety of dynamical influences can indicate the time since the pair was created. To date, no asteroid pairs have been found in the Jovian Trojans, despite the presence of several binaries and collisional families in the population. The search for pairs in the Jovian Trojan population is of particular interest, given the importance of the Trojans as tracers of planetary migration during the Solar system's youth. Here we report a discovery of the first pair, (258656) 2002 ES_{76} and 2013 CC_{41}, in the Jovian Trojans. The two objects are approximately the same size and are located very close to the L4 Lagrange point. Using numerical integrations, we find that the pair is at least 360 Myr old, though its age could be as high as several Gyrs. The existence of the (258656) 2002 ES_{76}–2013 CC_{41} pair implies there could be many such pairs scattered through the Trojan population. Our preferred formation mechanism for the newly discovered pair is through the dissociation of an ancient binary system, triggered by a sub-catastrophic impact, but we can not rule out rotation fission of a single object driven by YORP torques. A by-product of our work is an up-to-date catalogue of Jovian Trojan proper elements, which we have made available for further studies.

Key words: minor planets, asteroids: general – methods: numerical.

1 INTRODUCTION

The discovery of asteroid pairs, two objects sharing a very similar heliocentric orbit, recently brought yet another piece of evidence into the mosaic of small Solar system bodies' evolution on short time-scales (e.g. Vokrouhlický & Nesvorný 2008). Examples of these couples have been found in the Main belt and Hungaria populations (Vokrouhlický & Nesvorný 2008; Pravec & Vokrouhlický 2009; Rożek, Breiter & Jopek 2011; Pravec et al. 2019). The similarity between the heliocentric orbits of the two members of an identified asteroid pair hints at a common and recent origin for the objects, that most likely involves their gentle separation from a parent object. Indeed, backward orbital propagation of heliocentric state vectors of the components in many pairs has allowed researchers to directly investigate the possibility of their past low-velocity and small-distance approach (see Vokrouhlický et al. 2017, for the most outstanding example discovered so far).

The well-documented cases of pairs among asteroids identified to date all feature separation ages of less than a million years. Vokrouhlický & Nesvorný (2008) speculated about three processes that could have led to the formation of those paris: (i) collisional break-up of a single parent object, (ii) rotational fission of such an object driven by radiation torques, and (iii) instability and separation of the components of a binary system. Whilst each of these possibilities can explain the origin of asteroid pairs, with some being more likely than others for individual pair cases, evidence has been found that the majority of currently identified pairs were probably formed through the rotational fission of their parent object (e.g. Pravec et al. 2010, 2019). It is worth noting that Main belt binaries in the same size category (i.e. with primary diameters of one to a few kilometers), are also believed to be primarily formed through the rotational fission of their parent body (e.g. Pravec & Harris 2007; Margot et al. 2015a). This is an interesting population-scale result that informs us about a leading dynamical process for few-km size asteroids in the Main belt. It would certainly be desirable to extend this knowledge to other populations of small Solar system bodies.

Attempts to detect orbital pairs in other populations have, to date, either failed or were not strictly convincing. For instance, the orbital evolution of bodies in the near-Earth population is very fast and chaotic and, at the same time, the number of known objects is limited (see e.g. Moskovitz et al. 2019, and references therein). Searches in populations beyond the Main belt were not successful for different reasons. Whilst dynamical chaos could also be relevant, a more important factor concerns the smallest size of bodies found at larger distance from the Sun. The smallest bodies found in Cybele zone, and amongst the Hildas or Jovian Trojans, are about an order of magnitude larger than the smallest known asteroids in the inner Main belt or the Hungarias (e.g. Emery et al. 2015). The proposed pair-formation processes have a characteristic time-scale that rapidly increases as a function of parent body size. For that reason, it is no surprise that, to date, no recently formed ($\lesssim$1 Myr) traditional pairs sharing the same heliocentric orbit have been detected beyond the Main belt. If any pairs do exist in these distant small-body

★ E-mail: timothy.holt@usq.edu.au

populations, they should be revealed by their tight configuration in proper element space and long-term backward orbital propagation, if the stability in that particular zone of orbital phase space allows. With that guideline in mind, we focus here on the Jovian Trojan population. The leap to the Trojan population might appear to contradict the logical steps of gradually extending our knowledge of Main belt pairs by searches among the Cybele or Hilda populations first. However, we argue that the case of possible Jovian Trojan pairs is actually more interesting because of that population's entirely different origin.

The Jovian Trojan population consists of two swarms of objects, librating on tadpole trajectories about the Jovian L4 and L5 Lagrange points. Indeed, 588 Achilles Wolf (1907) was the first discovered object to serve as an example of a solution to the restricted three-body problem (Lagrange 1772). Whilst originally considered to be just an extension of the main belt, and particularly the Hilda and Thule populations, towards the orbit of Jupiter, the Jovian Trojans were soon realized to be a totally distinct group of objects, with a unique history (see Emery et al. 2015, for a review). Most importantly, the majority of the Jovian Trojans are thought to have formed in a vast trans-Neptunian disc of planetesimals, at a heliocentric distance beyond $\simeq$20 au, and became captured on to their current orbits during the planetesimal-driven instability of giant planets (see Nesvorný 2018, for review). The physical properties of the Trojans, such as their material strength or bulk density, are therefore most likely different from most of the asteroidal populations, resembling rather those of comets and Centaurs with which they share the birth-zone. Though relatively stable, the Jovian Trojans can escape their stable region (e.g. Di Sisto, Ramos & Beaugé 2014; Holt et al. 2020, and references therein), and contribute to other populations, most notably the Centaurs (see Di Sisto, Ramos & Gallardo 2019, and references therein). An example of this, (1173) Anchises, exhibits significant dynamical instability on time-scales of hundreds of millions of years, with the result that it will likely one day escape the Jovian Trojan population and become a Centaur before being ejected from the Solar system, disintegrating, or colliding with one of the planets (Horner, Müller & Lykawka 2012).

Despite their importance as a source of information on the Solar system's past evolution, fact that the Jovian Trojans are markedly farther from Earth than the Main Belt has made them significantly more challenging targets for study. As a result, our knowledge of the collisional history, binarity, and the presence/absence of pairs in the Trojan population remains far smaller than our knowledge of the main Asteroid belt (e.g. Margot et al. 2015b). In fact, to date, no confirmed Trojan pairs have been discovered, and the true level of binarity in the population remains to be uncovered. The most famous confirmed binary in the Trojan population is (617) Patroclus, accompanied by a nearly equal size satellite Menoetius (both in the 100 km range; e.g. Marchis et al. 2006; Buie et al. 2015). The Patroclus–Menoetius system is fully evolved into a doubly synchronous spin–orbit configuration (see Davis & Scheeres 2020, and references therein), and represents an example of the kind of binary systems which are expected to be common among Trojans. A number of such binaries, comprising two components of almost equal size, have been found amongst the large trans-Neptunian objects (e.g. Noll et al. 2020). This comparison is of particular interest, given that the Patroclus system was, in all likelihood, implanted to the Trojan region from the trans-Neptunian region source zone (e.g. Nesvorný et al. 2018). It seems likely that the Patroclus system represents the closest example of an Edgeworth-Kuiper belt binary system. Further information on the Patroclus system will become available in the coming decades, as the binary is a target for flyby in 2033 by the *Lucy* spacecraft (e.g. Levison et al. 2017). Similar smaller scale systems may well exist among the Trojan population, but their abundance is uncertain. Observationally, such small-scale binaries remain beyond our detection, and theoretical models of their survival depend on a number of unknown parameters (e.g. Nesvorný et al. 2018, 2020; Nesvorný & Vokrouhlický 2019). The existence of Trojan binaries is interesting by itself, but in the context of our work, it is worth noting that, if such binaries exist, they likely serve as a feeding cradle for a population of Trojan pairs.

Following this logic, then if the population of pairs among the Trojans can become known and well characterized, such that their dominant formation process is understood, that would in turn prove to be a source of new information about Trojan binaries. Milani (1993) in his pioneering work on Jovian Trojan orbital architecture noted a case of L4-swarm objects (1583) Antilochus and (3801) Thrasymedes. Their suspicious orbital proximity led the author to suggest that they may constitute a genetically related couple of bodies. A viable formation process would be through the instability and dissociation of a former binary (Milani and Farinella, personal communication). Unfortunately, the Antilochus–Thrasymedes interesting configuration has not since been revisited, nor further studied in a more detail.

This background information motivates us to conduct a search for Jovian Trojan pairs. Unfortunately, even now the problem is not simple, and we consider our work to be an initial attempt, rather than providing a definitive solution. In Section 2, we explain our strategy, and describe the difficulties in Trojan pair identification. This strategy led us to preliminarily identify the Jovian Trojans (258656) 2002 ES_{76} and 2013 CC_{41} as a potential pair. To test this hypothesis, we attempted to prove that these two bodies could be genetically related using backward orbital integration, as described in Section 3. In Section 4, we discuss potential formation processes for the pair, before presenting our concluding remarks and a call for observations in Section 5. Appendix A describes our methods for the construction of Jovian Trojan proper elements. An up-to-date catalogue of those elements, which we have made publicly available online, is actually a fruitful by-product of our work that may prove useful for future studies. We discuss some additional candidate pairs in Appendix B.

2 SELECTION OF CANDIDATE PAIRS

The discovery of asteroid pairs was a direct by-product of a search for very young asteroid families (see Nesvorný & Vokrouhlický 2006; Nesvorný, Vokrouhlický & Bottke 2006; Vokrouhlický & Nesvorný 2008). As a result, the primary ambition was to find pairs that formed recently, within the last Myr, amongst the Main belt and Hungaria populations. In fact, the necessity for proven pairs to be young is essentially related to the method that allows their identification.

Just like collisional families, asteroid pairs are identified as a result of the similarity of their heliocentric orbits. The search for classical collisional families has traditionally been performed using clustering techniques in proper orbital element space, examining the proper semimajor axis a_P, eccentricity e_P, and the sine of proper inclination $\sin I_P$ (see e.g. Benjoya & Zappalà 2002; Nesvorný, Brož & Carruba 2015, for reviews). The use of the proper elements allows us, with some care, to search for both young and old families. This is because the proper elements are believed to be stable over much longer time-scales than other types of orbital elements, such as osculating or mean, ideally on a time-scale reaching hundreds of Myrs or Gyrs.

There are, however, limitations to this method. In the case of very old families, problems arise from instability of the proper orbital elements and the incompleteness of the dynamical model used to

derive the proper elements. A different problem occurs for very young families. The issue has to do with the huge increase in the number of small-body objects discovered over the past decades. Despite the fact that the very young families and asteroid pairs must have very close values of the proper orbital elements, it is difficult to statistically discern them from random fluctuations of background asteroids. Both occur at the same orbital distance in proper element space.

This fundamental obstacle arises due to the low dimensionality of proper element space, which consists of just three independent variables. In order to separate very young asteroid families and asteroid pairs from the random fluctuations of the background population, Nesvorný, Vokrouhlický & Bottke (2006) and Vokrouhlický & Nesvorný (2008) realized that this problem can be overcome if the search is conducted in a higher dimensional space. As a result, they used the 5D space of the osculating orbital elements, neglecting just the mean longitude. The mean orbital elements are also suitable alternative parameters for such an analysis (e.g. Rożek, Breiter & Jopek 2011). In order to effectively use the two extra dimensions, the searched structures must also be clustered in secular angles, the longitudes of ascending node and perihelion. This is perfectly justified for very young families and pairs that are expected to have separated at very low velocities.

Previous searches for these young structures in the space of osculating or mean orbital elements proved the usefulness of the method, provided the age of the pair was less than about 1Myr. Asteroid pairs will clearly exist that formed earlier than this limit, but a differential precession of their secular angles will result in them becoming effectively randomized, which will, in turn, render the identification procedure described above ineffective. A key point here is that the population of Main belt asteroids is currently known to very small sizes, with objects detected with diameters of 1 km, or even smaller. The proposed formation processes for very young families and pairs are expected to generate enough pairs within the last Myr that, even after accounting for discovery biases, we still have some of them in our catalogues.

The situation is, however, different in the case of the Jovian Trojan swarms. First, the characteristic size of the smallest Trojans is $\simeq$5 km, with few objects being discovered that are smaller than this limit. Secondly, the formation processes of putative Trojan pairs, such as a rotational fission or collisions, are significantly less efficient than in the main belt. As a result, no identifiable pairs among Trojans are expected to have been formed in the last 10–30 Myr, over which time, one would expect secular angles of any such pairs to diverge from each other. We conducted a traditional search for pairs in the 5D space of osculating orbital elements (as in Vokrouhlický & Nesvorný 2008), but did not find any candidates. If pairs do exist amongst the known Trojans, their ages must be larger. In that case, however, their secular angles would be randomized, as is the case for old pairs in the main belt. Our candidate selection method then returns back to the analysis of the Trojan proper elements, with further considerations based on additional criteria.

2.1 A new catalogue of proper orbital elements

The AstDyS website, founded at the University of Pisa, and currently run by SpaceDys company (see https://newton.spacedys.com/astdys/), is a world renowned storehouse of proper orbital elements for Solar system minor bodies. It also contains data on the Jovian Trojans, namely synthetic proper elements based on mathematical methods presented in the pioneering work of Milani (1993). We also note the work of Beaugé & Roig (2001), which discusses an alternative approach to the calculation of Trojan proper elements, but these authors neither make their results readily available online, nor update them on a regular basis. For that reason, one possibility for this study would be to use the AstDyS data. However, those data have at least two drawbacks for our application. First, their last update occurred in 2017 June. As a result, they provide information for a total of 5553 numbered and multi-opposition Jovian Trojans. Given the efficiency of all-sky surveys, this number has increased significantly in the years since that update, with more than 7000 Jovian Trojans now known for which observations span multiple oppositions. Secondly, the proper elements provided at AstDyS are given to a precision of just four decimal places, which is not sufficient for our work. The AstDyS data base would, as a result, allow the determination of the orbital distance in the proper element space – equation (1) – with only $\simeq$2 to 5 m s^{-1} accuracy, which is insufficient to characterize the low velocity tail. For both of these reasons, in this work, we decided to determine our own synthetic proper elements. Details of the approach are given in Appendix A. Here, we only mention that our proper element definition and mathematical methods follow the work of Milani (1993), with substantial differences only for those orbits with very small libration amplitudes. Previous applications using this technique may be found in Brož & Rozehnal (2011) and Rozehnal et al. (2016).

Fig. 1 shows our results, namely proper elements computed for 7328 Jovian Trojans (numbered and multi-opposition objects as of 2020 April) projected on to the ($da_{\rm P}$, $\sin I_{\rm P}$) and ($da_{\rm P}$, $e_{\rm P}$) planes for the L4 swarm ('Greeks' leading Jupiter on its orbit; left-hand panels) and the L5 swarm ('Trojans' trailing behind Jupiter; right-hand panels). The L4 swarm is more numerous, partly as a result of four major collisional families that have been recognized in recent years (e.g. Rozehnal et al. 2016), and contains 4607 objects. The smaller L5 swarm contains only 2721 known objects, including the 2001 UV$_{209}$ and Ennomos collisional families. To proceed with an investigation of the orbital similarity between members of the Trojan population, the basis of the pair and family recognition process, one must introduce a metric function in the space of the proper orbital elements. Several choices have been discussed by Milani (1993). We opt for the d_3 metric, also favoured by the author of that work, though we slightly adjust that metric, such that the orbital distance is given in velocity units. Given two orbits in the Trojan L4 or L5 proper element space, obviously without mixing the two swarms, we define their distance $\delta V_{\rm P}$ as a quadratic form using the differences $\delta a_{\rm P}$, $\delta e_{\rm P}$, and $\delta \sin I_{\rm P}$ as

$$\delta V_{\rm P} = V_{\rm J}\sqrt{\frac{1}{4}\left(\frac{\delta da_{\rm P}}{a_{\rm J}}\right)^2 + 2\,(\delta e_{\rm P})^2 + 2\,(\delta \sin I_{\rm P})^2}, \qquad (1)$$

where $V_{\rm J} \simeq 13\,053$ m s^{-1} and $a_{\rm J} \simeq 5.207$ au are mean orbital velocity and semimajor axis of Jupiter. Milani (1993) argued that this particular choice of the coefficients – (0.25,2,2) – helps to equally weight contributions from all three dimensions.

2.2 Metrics-based analysis

Given the metric shown in equation (1), we computed distances of all possible pairs in the L4 and L5 Trojans swarms, and organized them in the form of a cumulative distribution $N(< \delta V_{\rm P})$ (see also Vokrouhlický & Nesvorný 2008, for context). The results of this process are shown in Fig. 2. Whilst the largest $\delta V_{\rm P}$ values of approximately $V_{\rm J}$ are set by the maximum extension of the stable phase space of tadpole orbits associated with Jupiter (Fig. 1), the smallest $\delta V_{\rm P}$ values of the order of $\sim$1–2 m s^{-1} are determined by a

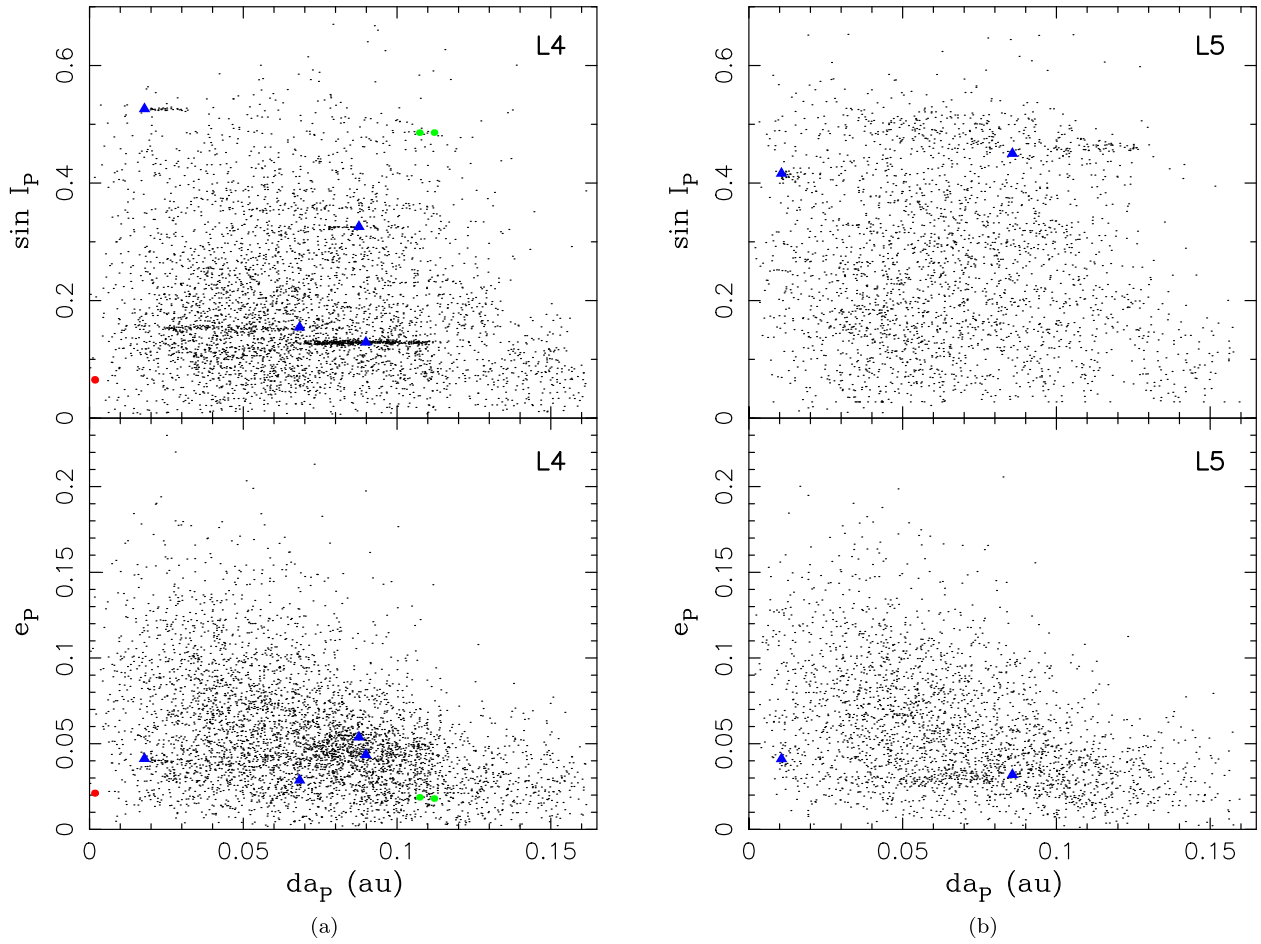

Figure 1. Proper orbital elements of Jovian Trojans: semimajor axis da_P versus sine of inclination sin I_P (top panels), and semimajor axis da_P versus eccentricity e_P (bottom panels). the left panels show the orbits of 4607 objects at the L4 libration zone, whilst the right panels show the orbits of 2721 objects at the L5 libration zone. These data were computed using the method described in Appendix A and display numbered and multi-opposition orbits as of April 2020. Blue triangles indicate the largest objects of the previously identified Trojan families (e.g. Rozehnal et al. 2016): (a) Eurybates, Hektor, Arkesilaos and 1996 RJ in the L4 zone, and (b) Ennomos and 2001 UV_{209} in the L5 zone. The two green circles denote position of Jovian Trojans (1583) and (3801) that were previously identified as constituting a suspiciously close pair (see Milani 1993). The two overlapping red circles denote the location of our proposed pair candidate of (258656) 2002 ES_{76} and 2013 CC_{41}.

combination of several factors. The number of known Jovian Trojans filling the stable orbital space is the first factor, compared with the typical smallest values $\delta V_P \simeq 100$ m s^{-1} found by Milani (1993), who studied just 80 and 94 Trojans in the L4 and L5 swarms, respectively. Additionally, small velocity differences occur when bodies become organized in structures like families. Last, the inevitable uncertainty of the proper elements contributes to the noise in δV_P. We determine the uncertainties of δV_P by a propagation of the proper element uncertainties described in Appendix A. This effect is obviously not uniform, but organized in a complicated structure of a chaotic web, generally increasing towards the border of the stable tadpole zone (see e.g. Robutel & Gabern 2006). Interestingly, the characteristic noise level from such deterministic chaos is of the order of a few meters per second, about the same as minimum distances between the orbits, as can be seen in Fig. 2, where we show uncertainty intervals of δV_P for the low-velocity tail.

It is also worth noting that for reasonably small values of δV_P (hundred m s^{-1} or so), one would expect $N(<\delta V_P) \propto (\delta V_P)^3$ provided that: (i) Trojans fill the available stable phase space at random, and (ii) the weighting coefficients in the metric function (1) truly express isotropy, the exponent 3 is then a measure of the proper element space dimension. For large δV_P values the cumulative distributions $N(<\delta V_P)$ become shallower because of the finite extent of the stable orbital region. We also note that $N(<\delta V_P)$ holds global information about the whole L4 and L5 populations, while local structures, such as families and clusters, are almost not seen in this distribution.

We find it interesting that $N(<\delta V_P)$ are broadly similar for the L4 and L5 swarms, but they also differ in some important characteristics, in particular, the smallest and the largest δV_P values. This is due to the directly comparable populations of the two swarms and basically identical volumes of their stable phase space. However, the $\delta V_P < 100$ m s^{-1} parts of the distributions have a different behaviour when approximated with a power-law $N(<\delta V_P) \propto (\delta V_P)^\alpha$: (i) the L4 swarm has the canonical value $\alpha \simeq 3$, while (ii) the L5 swarm is shallower, with approximately $\alpha \simeq 7/3$. We hypothesize that this difference is caused by a presence of the prominent Trojan families in the L4 population. Family members efficiently contribute to the low-δV_P part of the distribution. Given their small extent, it is also conceivable that the mutual orbital distribution in families is approximately isotropic. The L5 population is less influenced by Trojan families, and, as a result, $N(<\delta V_P)$ may reflect the parameters of the background Trojan population. This is affected both by the resonances that sculpt the

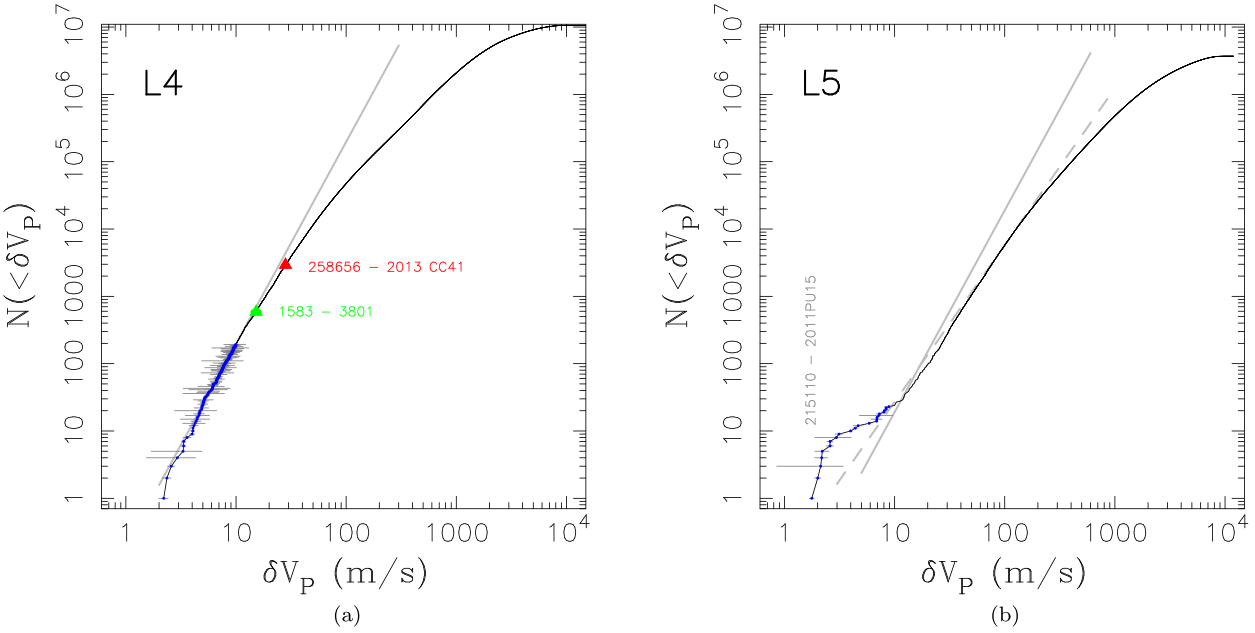

Figure 2. Cumulative distribution $N(< \delta V_P)$ of Trojans with velocity distance δV_P in the proper elements space using the metric described in equation (1): the left-hand panel presents the results for the 4607 objects of the L4 Trojan swarm, with the right-hand panel showing the 2721 members of the L5 Trojan swarm. The light grey solid lines indicate the $N(< \delta V_P) \propto (\delta V_P)^3$ relationship, for reference; curiously, the L5 distribution is better matched with $N(< \delta V_P) \propto (\delta V_P)^{7/3}$, shown with a dashed grey line. The blue symbols denote the population with the smallest δV_P values, namely $\delta V_P \leq 10\,\mathrm{m\,s^{-1}}$ for both the L4 and L5 Trojans. For sake of interest, we also show uncertainties in the determination of δV_P for these low-velocity couples with grey horizontal intervals. Position of three couples of interest is highlighted by labels. These are the (1583)-(3801) couple with $\delta V_P = (15.2 \pm 1.0)\,\mathrm{m\,s^{-1}}$ and (258656) 2002 ES_{76}–2013 CC_{41} couple $\delta V_P = (28.2 \pm 0.9)\,\mathrm{m\,s^{-1}}$ among L4 Trojans, and (215110) 1997 NO_5–2011 PU_{15} couple with $\delta V_P = (1.8 \pm 0.1)\,\mathrm{m\,s^{-1}}$ among L5 Trojans.

stable orbital zone in a complicated way and, perhaps, the initial filling of the Trojan region by planetesimals. Finally, the weighting coefficients of the metric function (1), that express how differences in semimajor axis, eccentricity, and inclination contribute to the whole, may also slightly affect the result (though our experiments with small changes in those values did not yield significant differences). If combined altogether, the α value may be slightly shallower than 3, such as 7/3 we found for the L5 population

We paid some attention to the smallest-distance couple (215110) 1997 NO_5–2011 PU_{15}, and could not conclusively prove that it represents a real pair of related objects (Appendix B). A closer analysis of the second to sixth closest couples in the L5 population indicates the possibility of a very compact cluster about Trojan (381148) 2007 GZ_1, but its status needs to be confirmed with more data in the future. In any case, because our interest here focuses on Trojans in the low-velocity tail of the $N(< \delta V_P)$ distribution, seeking putative pairs, we also show in Fig. 3 location of couples that have $\delta V_P < 10\,\mathrm{m\,s^{-1}}$ in both Trojan swarms. These would be the most logical candidates for further inspection.

Seeking details that could explain the difference in the population exponents α in further detail, we analysed distributions of the proper elements. The most significant difference concerns proper inclination I_P. Fig. 4 shows L4 and L5 Trojan distributions of I_P for all bodies. The dashed lines are simple approximations with a function $I_P \exp(-I_P/C)$, where the adjustable constant C characterizes width of the distribution (the prominent families, such as Eurybates at $\simeq 8^\circ$ among L4 or Ennomos at $\simeq 30^\circ$ among L5, were excluded from the fit). We found $C \simeq 6.0^\circ$ for L4 and $C \simeq 8.7^\circ$ for L5, implying the inclination distribution at L5 is slightly broader. This confirms results in Di Sisto, Ramos & Beaugé (2014). It is not clear, whether this is due to the details of the capture process, or whether the escapees from the prominent Eurybates and Arkesilaos families in the L4 swarm contribute to the difference, and how it may affect the exponent α of the $N(< \delta V_P)$ distribution discussed above. A full analysis of these interesting findings is beyond the aims of our work. Regarding the smallest δV_P values, neither of the two distribution functions $N(< \delta V_P)$ show a change in behaviour. In the context of our work, this implies no hint of a statistically significant population of very close orbits, a tracer of a possible Trojan pair population. In fact, given the low dimensionality of the proper element space, this was not unexpected, given that the asteroid pairs in the Main belt would not manifest themselves using a similar analysis. The slight deviation of $N(< \delta V_P)$ below $\simeq 7\,\mathrm{m\,s^{-1}}$ velocity to a shallower trend for the L5 swarm is interesting, but likely not statistically robust enough to allow firm conclusions to be drawn at the current time.

A full frontal approach to this data would be to analyse the results from backward orbital integrations for these little more than 200 putative couples using the methods described in Section 3. However, this would require a significant computational effort, and thus we chose to adopt further criteria for candidate selection. For instance, data in the L4 swarm show that the lowest δV_P couples are strongly concentrated in the recognized families. The locally increased density of Trojans in these regions obviously imply small distances δV_P, but this also means such couples are most likely not the objects that we seek. The correlation with Trojan families is somewhat weaker in the L5 swarm, though several of the small-distance couples are found in both the Ennomos and 2001 UV_{209} families. Other constitute compact clusters scattered in the background population, like that around (381148) 2007 GZ_1, as mentioned above.

Sifting the $\delta V_P < 10\,\mathrm{m\,s^{-1}}$ couples unrelated to families would still leave us with too many candidates to pursue with backward n-body

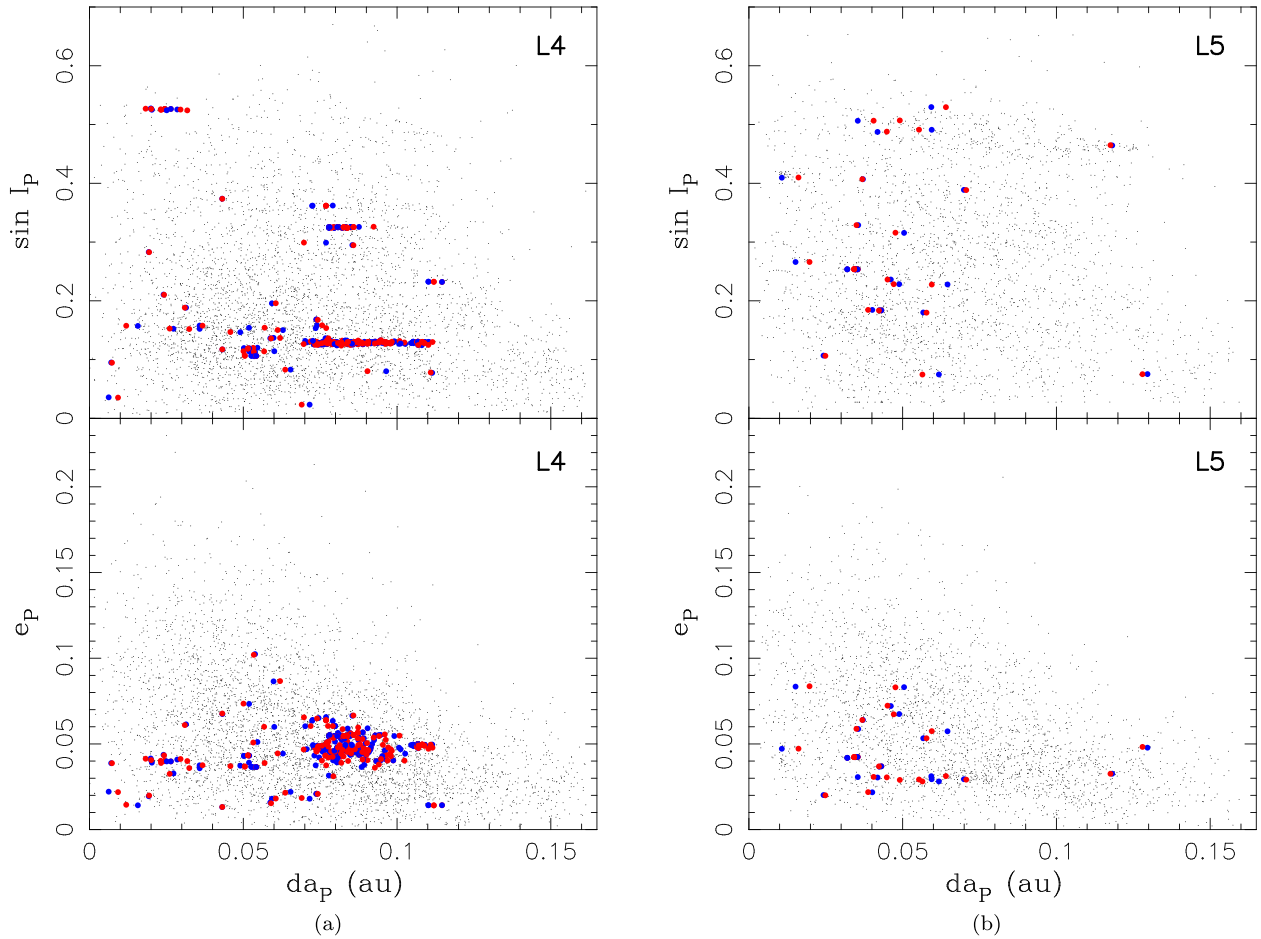

Figure 3. Proper orbital elements of Jovian Trojans as in Fig. 1. The red symbols in both L4 and L5 swarms show couples of Trojans with $\delta V_P < 10\,m\,s^{-1}$, namely the lowest velocity tail in the distributions shown in Fig. 2: the primary component of each couple is shown using a filled red circle, whilst the secondary is shown using a blue circle. In the L4 case their relation to the recognized families is apparent. In the L5 case their distribution is more scattered, though some are also associated with the 2001 UV_{209} and Ennomos families.

simulations. Having experimented with several cases, we adopted the strategy of focusing on those low-δV_P couples characterized by (i) the least populated background, and (ii) located in the most dynamically stable zones of the orbital phase space. The former condition increases the likelihood that the candidate couple is a real pair, and not just a fluke, whilst the latter condition would allow us to investigate the past orbital configuration of the putative pair across as lengthy a time-scale as possible. This is particularly important for pairs in the Jovian Trojan population, since no recently formed pairs are to be expected, as described above. Moreover, the expected large ages of possible Trojan pairs do not allow us to seek their past orbital convergence in full 6D Cartesian space of positions and velocities. Even the most stable Trojan orbits have an estimated Lyapunov time-scale of about 10–20 Myr. In this situation, our convergence scheme should rely on the behaviour of secular angles, the longitudes of node and perihelion, and the related eccentricity and inclination (Section 3). It is then advantageous to suppress the role of the last two elements, the semimajor axis, and the mean longitude, by letting them vary as little as possible. This favours locations very near the tadpole libration centre of either the L4 or L5 swarms, where also the previous two conditions, low background population and maximum orbital stability, are satisfied.

2.3 A prospective candidate Trojan pair

With all these criteria in mind, we found a candidate couple of L4 objects, (258656) 2002 ES_{76} and 2013 CC_{41}. The proximity of these two objects to the libration centre is reflected by the small values of all proper elements (see Fig. 1), namely $da_P \simeq (1.6180 \pm 0.0001) \times 10^{-3}$ au, $e_P \simeq (2.12713 \pm 0.00001) \times 10^{-2}$, and $\sin I_P \simeq (6.578 \pm 0.003) \times 10^{-2}$ for (258656) 2002 ES_{76}, and $da_P \simeq (1.6890 \pm 0.0001) \times 10^{-3}$ au, $e_P \simeq (2.10588 \pm 0.00001) \times 10^{-2}$ and $\sin I_P \simeq (6.427 \pm 0.004) \times 10^{-2}$ for 2013 CC_{41}. The close proximity to L4 also indicates that the pair have been in stable orbits for the life of the Solar system (e.g. Holt et al. 2020). For reference, we also mention their libration amplitude, in the angular measure, which is only about 0.33°, resp. 0.34°. There are only four other L4 objects in our sample that have smaller libration amplitudes, and none among the known L5 objects, though these have generally larger proper eccentricity and/or inclination values. The similarity of the two orbits is immediately apparent and quantitatively expressed with $\delta a_P \simeq 7.1 \times 10^{-5}$ au and $\delta e_P \simeq 2.12 \times 10^{-4}$, both with negligible uncertainty, while $\delta \sin I_P \simeq 1.51 \times 10^{-3}$ with a small uncertainty of 4.8×10^{-5}. This uncertainty amounts to about 0.085° difference in the proper inclination. All these values result in the velocity difference $\delta V_P \simeq 28.2 \pm 0.9\,m\,s^{-1}$, using our adopted metric (1),

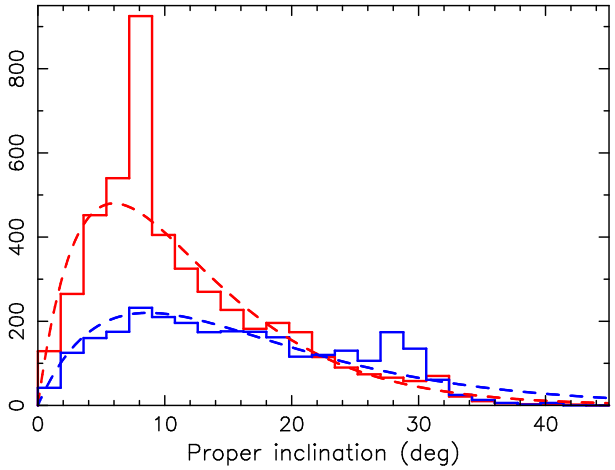

Figure 4. Number of Jovian Trojans with proper inclination I_P (in degrees), showing the L4 (red) and L5 (blue) swarms. The dashed lines represent an approximation $I_P \exp(-I_P/C)$ for the background population (significant peaks due to Trojan families eliminated), where we found $C \simeq 6.0^\circ$ for L4 and $C \simeq 8.7^\circ$ for L5.

dominated by the inclination contribution the contribution from the difference in proper eccentricities is about 10 per cent of the total, and the difference in proper semimajor axes is negligible). With that said, this couple would qualify among the closest in the population if it were not for the slight inclination offset of the two orbits.

Not much physical information is available about these two objects. Various data bases providing orbital solutions (such as AstDyS, JPL, or MPC) yield an absolute magnitude for (258656) 2002 ES_{76} in the range 14.0 to 14.2, and values in the range 14.3 to 14.4 for 2013 CC_{41}. Given the mean albedo, $p_V \simeq 0.075$, for small Trojans (a value with an admittedly large scatter; e.g. Grav et al. 2011, 2012), we estimate their sizes to be $D \simeq 7.0$–7.7 km for (258656) 2002 ES_{76} and $D \simeq 6.4$–6.7 km for 2013 CC_{41}. Unless the assumption of similar albedoes is significantly in error, it is clear that the two bodies are similar in size, though not exactly the same. No other physical parameters, such as the rotation period, thermal inertia, and/or spectral colours, are known at the present time. Further observational follow-up on these objects is therefore highly recommended.

2.4 Assessment of the statistical significance of the selected pair

The small libration amplitude zone of the proper element space contains a relatively small number of bodies, as can be seen in the left-hand panel (a) in Fig. 5. Here, we used the range $da_P \leq 0.014$ au, expressing the proximity to the libration centre, but left $e_P \leq 0.15$ and $\sin I_P \leq 0.6$, generally capturing the width of the stable Trojan phase space (Levison, Shoemaker & Shoemaker 1997; Nesvorný et al. 2002a; Tsiganis, Varvoglis & Dvorak 2005; Di Sisto et al. 2014; Holt et al. 2020). We could have also more strongly restricted the proper eccentricity and inclination values, but if this is done too aggressively, it would result in the sample of observed Trojans available for our analysis becoming too small. With our limits, we find $k = 91$ Trojans in the L4 space, including our candidate pair (258656) 2002 ES_{76} and 2013 CC_{41}.

The proper element differences in the (258656) 2002 ES_{76} and 2013 CC_{41} couple are $\delta a_P = 7.11 \times 10^{-5}$ au, $\delta e_P = 0.000212$, $\delta \sin I_P = 0.00151$, much smaller than the scale of the chosen zone, assuming that all dimensions are taken equally. In the first approximation, taking all dimensions equally, and thus neglecting the weighting coefficients from equation (1) which are all of the order of unity, the (δa_P, δe_P, $\delta \sin I_P$) differences in this couple define a small box of which represents only a $\simeq 1.81 \times 10^{-8}$ fraction of the analysed target zone. For statistical calculations, it is useful to imagine 'numbered' boxes of the (δa_P, δe_P, $\delta \sin I_P$) volume in the whole zone. Their total number of such boxes would then be $n \simeq 5.53 \times 10^7$.

The simplest estimate of the statistical significance of the (258656) 2002 ES_{76}–2013 CC_{41} pair is based on the assumption that bodies were distributed in the analysed zone randomly/uniformly. We choose k numbers from n possibilities (i.e. one for each body from a set of 'numbered' boxes). Ordered, repeated selections are given as variations $V'(n, k) = n^k$, while ordered, non-repeated as $V(n, k) = n!/(n-k)!$. The likelihood that among the trials the box-numbers do not repeat is simply the ratio $V(n, k)/V'(n, k)$, and we are interested just in the complementary probability:

$$p = 1 - \frac{V(n,k)}{V'(n,k)} \simeq 7.4 \times 10^{-5}. \quad (2)$$

We verified this result by directly running a Monte Carlo simulation of the selection process. Thus, we find the probability that the selected couple is only a random orbital coincidence to be very low. Shrinking the width of the e_P and $\sin I_P$ to half the previously mentioned values did not change our result significantly.

As can be seen in the left-hand panel (a) of Fig. 5, the assumption of a uniform distribution of background Trojans in the target zone is fair, but not exactly satisfied. This is the result of the decreasing number of Trojans towards the libration centre (i.e. at very small values da_P). We therefore repeated our analysis in a different system of coordinates. Keeping e_P and $\sin I_P$, we now changed da_P with $S = 4\pi(da_P)^2$. The background reasoning is that the libration point, $da_P = 0$, represents a centre about which the tadpole orbits move in 3D. In a Cartesian view centred at L4 the radial coordinate is to be replaced with the surface area $S = 4\pi(da_P)^2$. Re-mapping and re-binning our analysis in the (S, e_P, $\sin I_P$) coordinate system, we obtained the situation shown in the right-hand panel (b) of Fig. 5. Whilst still keeping the same number $k = 91$ of Trojans in the analysed zone, their distribution is now more uniform. Given the new box-definition by the (258656) 2002 ES_{76} and 2013 CC_{41} couple, we now find the number of thus defined small boxes to be increased to $n \simeq 2.34 \times 10^9$. This is the result of the candidate couple's close proximity to the libration centre. As a result, the likelihood (equation 2) of the couple being just a fluke in a uniform distribution of objects now becomes smaller, namely $p \simeq 1.75 \times 10^{-5}$.

The probability p, defined and computed for the (258656) 2002 ES_{76}–2013 CC_{41} couple above, is appreciably small. It is both interesting and important to compare this result with the similarly defined quantity for other Trojan couples, especially amongst those that have a small δV_P distance in the metrics (1). This will tell us whether the probability p for (258656) 2002 ES_{76}–2013 CC_{41} is sufficiently small in absolute measure for the couple to be considered a true pair, whilst at the same time enabling our algorithm to better connect our p definition with the velocity metrics used above. Here we analyse the L4-swarm population, but the same approach could equally be applied to the L5 case.

The potentially complicated part of the procedure is that, for each selected couple, we have to (i) adapt the box size (δa_P, δe_P, $\delta \sin I_P$), and (ii) the zone size (Δa_P, Δe_P, $\Delta \sin I_P$), as well as the position to which the box size refers. The choice of the latter obviously varies because the local number density of bodies differs from place to place. In order to prevent excessively small boxes in one of the dimensions (as an example, due to an almost zero difference $\delta e_P \doteq 0$),

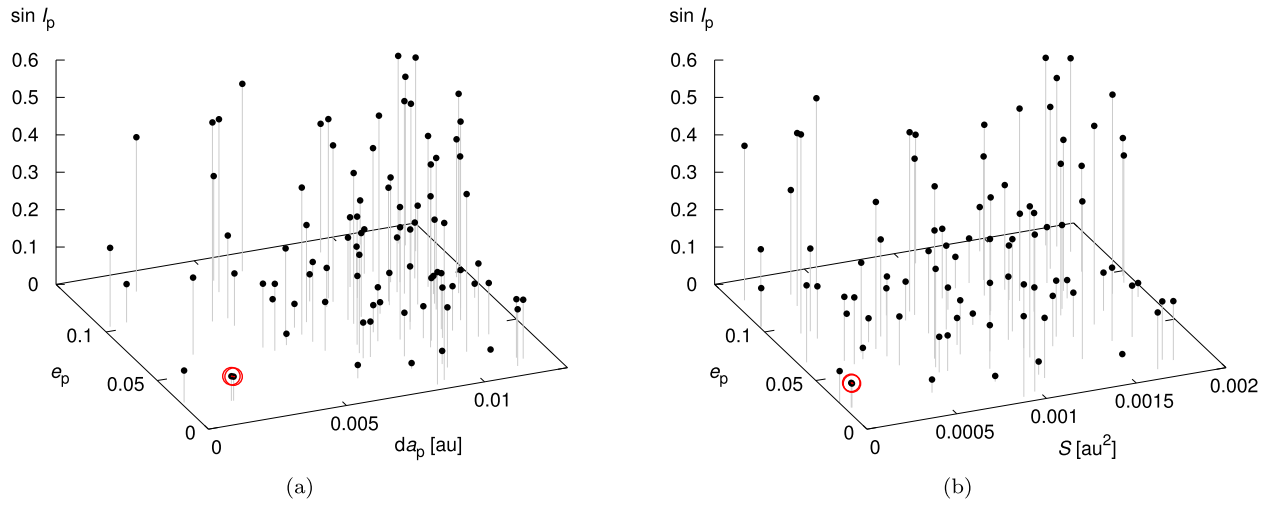

Figure 5. Left-hand panel (a): The small-libration portion of the L4 stable orbital zone in the 3D proper element coordinates (da_P, e_P, $\sin I_P$). The proximity to the libration was arbitrarily set by $da_P \leq 0.014$ au, whilst the extent of e_P and $\sin I_P$ is limited by orbital stability. We find 91 objects (black symbols) in this zone for our data set of Trojans. The candidate pair (258656) 2002 ES_{76} and 2013 CC_{41} is highlighted with a red circle. The vertical intervals help to appreciate 3D nature of the display. Right-hand panel (b): The same as on the left-hand panel, but the da_P was replaced with a surface area $S = 4\pi(da_P)^2$. In this case, the small-amplitude Trojans are distributed more uniformly.

we use the metric δV_P as a measure of the 'diagonal' of the box and we define its respective volume as $(\delta V_P)^3/\sqrt{3}$. Observing the typical spatial variation of the number density of Trojans, we use a fixed value for $\Delta a_P = 0.02$ au, rejecting pairs with $\delta a_P > 0.3\Delta a_P$. In order to prevent a low number of bodies k in the zone, both Δe_P and $\Delta \sin I_P$ are then sequentially increased until $k \geq 50$. Once we set the zone, we again define its volume as $(\Delta V_P)^3/\sqrt{3}$, with ΔV_P the velocity distance of the corners connected with a diagonal. The number of boxes n, as well as the probability p, is then computed as before (equation 2). Obviously, the whole algorithm cannot be done manually, but an automated computer script was written to run the method.

The statistical results of our analysis are shown in Fig. 6. The pairs seem to be well organized in the (p, δV_P) plane, expressing an overall correlation between the two quantities. As might be expected, the general trend is $p(\delta V_P) \propto (\delta V_P)^3$, namely volume of the box. Nevertheless, the p versus δV_P values do not follow a single curve, due to the local number density being different for each of the couples. Those couples located within known families generally have relatively high p values. This is to be expected, since the surrounding zones are densely populated by Trojans, which causes the dimensions of the zone to be small. To illustrate this effect, we coloured data for pairs in the largest families in the Fig. 6, identifying those in the (i) Eurybates family (blue), (ii) the core of the Hektor family (light blue), and (iii) the (9799) 1996 RJ family (cyan), after Nesvorný, Brož & Carruba (2015). The Eurybates family, the largest and most populous in the Trojan population, has systematically the largest p values. This is because even a small zone quickly contains our threshold number of $k = 50$ Trojans. We note that $p \simeq 1$, or even formally larger, just indicates that a couple of Trojans in this zone is fully expected at their distance δV_P. An exception to this rule is the (9799) 1996 RJ family, where we find the smallest p values, which are clearly correlated with δV_P. This is because (9799) 1996 RJ is a very compact family located in isolation in a high-inclination portion of the Trojan phase space (see also Fig. 1). For each of the couples selected in this family, the reference zone needs to be large to contain the minimum required number of objects.

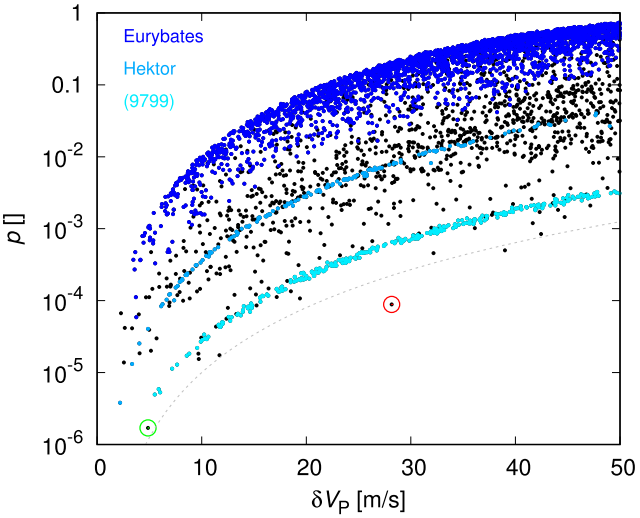

Figure 6. The probability p that a pair is random fluke, computed using the method described in the text, versus its distance δV_P, computed for all low-velocity pairs in the L4 zone using equations (2) and (1). The pair (258656) 2002 ES_{76} and 2013 CC_{41} is highlighted with a red circle. The pair (219902) 2002 EG_{134} and (432271) 2009 SH_{76}, discussed briefly in Appendix B, is highlighted with a green circle. The coloured symbols denote pairs in the identified L4 families: (i) Eurybates (blue), (ii) the core of the Hektor family (light blue), and (iii) (9799) 1996 RJ (cyan). The dashed line, $p = 10^{-5}\,(\delta V_P/(10\,\mathrm{m\,s^{-1}}))^3$, is used to emphasize that the candidate pair (258656) 2002 ES_{76} and 2013 CC_{41} is an outlier in this population.

Whilst the collisional families could clearly contain dynamical pairs, their recognition is confused by the locally high background of family members. We therefore exclude objects located in families from our work. What remains is then a diffuse background population of Trojans. For every fixed δV_P value, there are some background couples for which p extends to small values. The true Trojan dynamical pairs, namely those objects genetically related to a common parent, form the basis for our search among this population of a low-p tail for sufficiently small δV_P values. There are possibly a number of such

cases, but amongst them, the one which is the most outlying from the $p(\delta V_P) \propto (\delta V_P)^3$ reference level shown by the dashed curve in Fig. 6 is the case of (258656) 2002 ES_{76}–2013 CC_{41} (highlighted with red circle). Its p value is an order of magnitude lower when compared to couples with similar δV_P values. This justifies the validity of the (258656) 2002 ES_{76}–2013 CC_{41} couple as a true asteroid pair, based on our statistical analysis alone. There are also some family-unrelated couples with p values comparable or smaller, and these are briefly discussed in Appendix B.

In the next Section 3, we conduct a search for past orbital convergence of the selected (258656) 2002 ES_{76} and 2013 CC_{41} couple. If successful, this process adds an important piece of evidence justifying the couple as a real pair of genetically related objects. We explain our methods in detail. These methods are also briefly applied to several other candidate couples, with less success (Appendix B).

3 NUMERICAL SIMULATIONS

The dynamics of the Jovian Trojans have been extensively studied using both analytical and numerical means (e.g. Milani 1993; Beaugé & Roig 2001; Robutel & Gabern 2006; Di Sisto et al. 2014; Holt et al. 2020, and references therein). Here, we confine ourselves to briefly recalling only the information necessary for understanding and interpreting our numerical simulations of the (258656) 2002 ES_{76} – 2013 CC_{41} pair.

As previously noted, the objects in this pair are not typical, but are instead exceptional representatives of Trojan population. This is because they reside extremely close to the L_4 libration centre. As a result, the evolution of their semimajor axis a and the resonant argument $\lambda - \lambda_J$ be characterized by many small-amplitude and high-frequency terms. Those are, however, of the least importance for our analysis. More relevant is the behaviour of the eccentricity e, the inclination I, the longitude of ascending node Ω, and the longitude of perihelion ϖ. Due to the small values of the eccentricity and inclination, it is also useful to think about complex non-singular elements $z = e \exp(\imath \varpi)$ and $\zeta = \sin I \exp(\imath \Omega)$. In linear perturbation theory, a fairly satisfactory zero approximation, both z and ζ are represented by a finite number of Fourier terms, namely the proper term and a few forced planetary terms. A simpler description concerns ζ, whose Fourier representation is dominated by the proper term with $I_P \simeq 3.7^\circ$, followed only by small contributions from the s_6 term, with $I_6 \simeq 0.36^\circ$, and a number of significantly smaller contributions. As a result, the osculating inclination I is well represented by a constant I_P and a periodic term with amplitude I_6. Correspondingly, the osculating longitude of the ascending node, Ω, steadily circulates with a period given by the proper s frequency, and experiences only very small perturbation from the s_6 term. The evolution of z is more complicated because it is represented by three terms of comparable amplitude. The largest amplitude contribution, $\simeq$0.044, is provided by the term with frequency g_5, followed by proper g and g_6 terms with comparable amplitudes of $\simeq$0.021 and $\simeq$0.015. Whilst still very simple in the Cartesian representation of z, the polar variables in this plane (i.e. the eccentricity and especially longitude of perihelion) exhibit a non-linear evolution, characteristic of many low-eccentricity asteroid orbits.

3.1 Short-term simulations

Equipped with this knowledge, we can now turn to investigating the common origin of (258656) 2002 ES_{76} and 2013 CC_{41}. In studies of asteroid pairs, researchers seek to demonstrate a convergence of heliocentric orbits of the proposed pair at some moment in the past (e.g. Vokrouhlický & Nesvorný 2008). This is considered to be the origin of the two objects from a common parent body, and the corresponding time in the past representative of the age of the pair. As typically achievable ages of the asteroid pairs in the Main belt are less than 1Myr, with many less than 100 kyr, a convergence is often sought in Cartesian space. This approach means to demonstrate that the two orbits meet at the same point in space and have a very small relative velocity.

The same condition can be expressed in heliocentric orbital elements by making them basically equal at the formation moment of the pair. For this work, we find it markedly more useful to work with the orbital elements of our candidate pair, as they can teach us more readily about the evolution of the orbits of the two objects. Therefore, in Fig. 7, we show the results of our initial numerical experiment. We provide the differences between the osculating heliocentric elements of the nominal orbits of (258656) 2002 ES_{76} and 2013 CC_{41} over a short time interval of the past 10 Myr. We use the `swift_rmvs4` integrator (Levison & Duncan 1994) which allows us to efficiently include gravitational perturbations from all eight planets. The integration time-step used was 3 d, and the state vectors of all propagated bodies, planets, and the two Trojans, were output every 50 yr. We use a reference system defined by the invariable plane of the planetary system. The initial conditions of (258656) 2002 ES_{76} and 2013 CC_{41} at MJD58800 epoch were obtained from the `AstDyS` website.

The differences in the orbital elements shown in Fig. 7 oscillate with the dominant frequencies identified by the analysis of z and ζ themselves. For instance, the principal periodicity seen in δI and $\delta\Omega$ corresponds to the frequency $s_6 - s$, whilst the principal periodicity seen in δe and $\delta\varpi$ corresponds to frequencies g and $g_5 - g_6$. Differences δa and $\delta\lambda$ are characterized by higher frequencies, such as the planetary orbital frequencies, the libration frequency, and then followed by a 'forest' of lower frequencies starting with g.

We also note a markedly different behaviour of $\delta\varpi$ and $\delta\Omega$, which can be understood from the above mentioned description of the z and ζ non-singular elements of the two objects. Observing the general behaviour of the amplitude in the (δa, δe, $\delta\varpi$, $\delta\lambda$) terms, we note a curious fact that those amplitudes become very small simultaneously for semimajor axis, eccentricity, longitude of perihelion and longitude in orbit $\simeq$7.11 Myr ago (upper four panels in Fig. 7). However, any hope for a clear orbital convergence at that epoch is removed by looking at behaviour of the inclination and longitude of ascending node differences (bottom two panels in Fig. 7). We note that δI keeps steadily oscillating about a mean value of $\simeq -0.08^\circ$, namely a difference in the proper inclinations of (258656) 2002 ES_{76} and 2013 CC_{41}, without the amplitude of those oscillations showing any tendency to shrink. At the same time, the nodal difference stays large, and only slowly decreases from $\simeq -56^\circ$ to $\simeq -45^\circ$. This rate of decrease in $\delta\Omega$ fits perfectly the difference in proper frequencies s of the two objects as to be expected. Hence some $\simeq$7.11 Myr ago, the two orbits had basically identical (a, e, ϖ, λ) values, but the nodes were still offset by about 50°. This is inconsistent with any believable low-velocity separation of the two objects from a common parent body at their origin. Whilst inconclusive about the origin of the (258656) 2002 ES_{76} and 2013 CC_{41} couple, this 10 Myr integration provides useful hints for further analyses.

3.2 Long-term simulations

Extrapolating the trend seen in Fig. 7, we can estimate that the nodes of (258656) 2002 ES_{76} and 2013 CC_{41} became coincident some

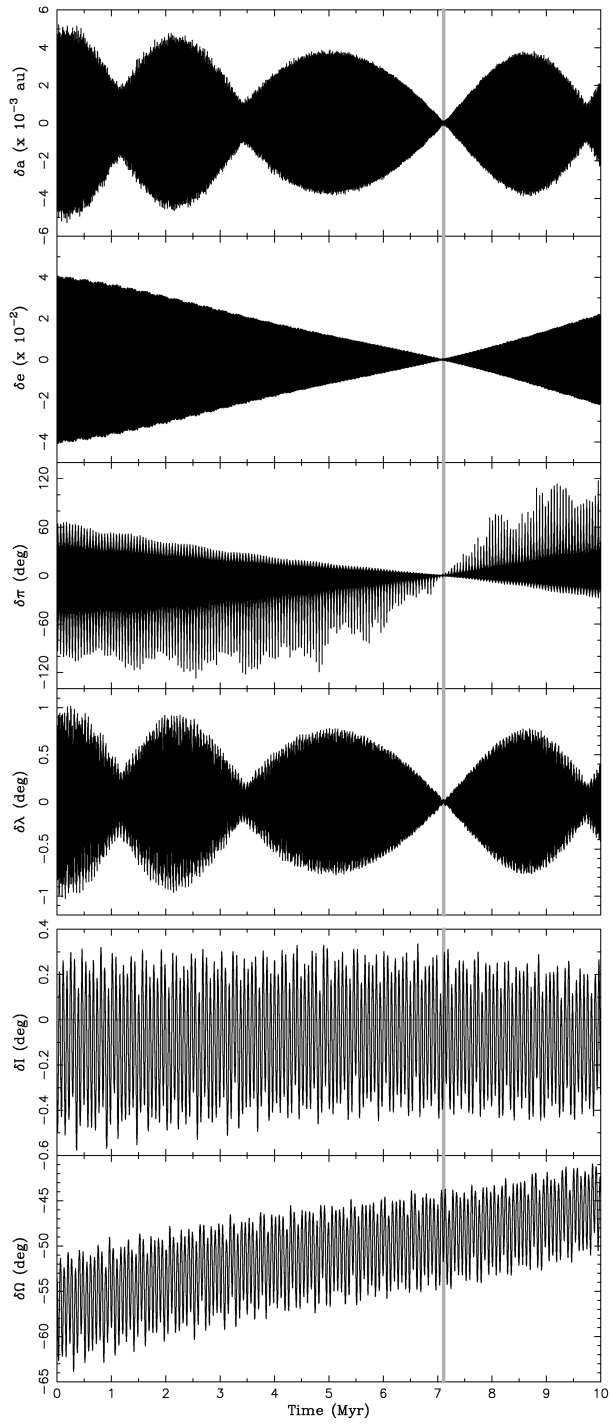

Figure 7. Differences between the osculating orbital elements of (258656) 2002 ES_{76} and 2013 CC_{41} from a 10 Myr backward integration of their nominal orbits. Gravitational perturbations from all planets were included and an invariable-plane reference system used. The differences of semimajor axis δa, eccentricity δe, longitude of pericentre $\delta\varpi$, and longitude in orbit $\delta\lambda$ (top four panels) indicate a simultaneous collapse to near zero values at $\simeq$7.11 Ma (grey vertical line). In contrast, the differences of inclination δI and longitude of ascending node $\delta\Omega$ (the bottom two panels) do not converge at that epoch: the nodal longitudes of the two objects are still $\simeq 50^\circ$ away from each other, and the inclination difference shows steady oscillation about the mean value of $\simeq -0.08^\circ$, namely a difference in their proper inclinations. The steady trend in $\delta\Omega$ has a slope $\simeq$0.004 arcsec yr^{-1}, very close to the difference in proper frequencies s of (258656) 2002 ES_{76} and 2013 CC_{41}.

50 Myr ago. Obviously, this is only the first such configuration in the historical evolution of the two objects. Assuming orbital stability, we also predict that the configuration will repeat with a $\simeq$320 Myr periodicity. To probe the long-term changes in the orbital architecture of the (258656) 2002 ES_{76}–2013 CC_{41} couple, we extended our previous simulation to 1200 Myr in the past. We note in passing that the necessity to seek this pair's age over such a long time-span forces us to abandon any hopes of finding a convergence in Cartesian coordinates. This is because of the small but non-negligible chaoticity of the integrated orbits, and principally results from an uncertainty in the thermal accelerations that the objects would experience (as discussed below). Both of these factors would require a large number of clones of (258656) 2002 ES_{76} and 2013 CC_{41} to investigate their past histories, and thus are computationally prohibitive to pursue. We therefore choose to downsize the dimensionality of the space where a convergence is quantified, and focus on the behaviour of secular evolution in just the non-singular elements z and ζ. Fig. 8 shows the differences between the osculating $\delta\Omega$ and $\delta\varpi$ of the two objects, and pays special attention to the time interval near $\delta\Omega \simeq 0$ configurations.

As expected, the first such configuration occurred about 50 Myr ago. However, a closer look at the relevant panel of Fig. 8 indicates that suitable orbital convergence conditions did not occur at that time. Unlike $\simeq$7.11 Mya, the orbital planes converge, but the perihelion longitudes are at the maximum of their oscillations. An even closer look at the epochs near nodal convergence shows that when $\delta\varpi$ crosses zero, δe is large, and vice versa. Once again, we therefore find that the conditions of a low-velocity separation of the two orbits cannot be met at that epoch.

Inspecting further epochs of nodal crossing, as shown in Fig. 8, we conclude that $\delta\Omega \simeq 0$ in fact never exactly coincides with $\delta\varpi \simeq 0$, a convergence pre-requisite. Here, however, we must revisit some of the assumptions made in our simulation. In particular, recall that (i) we used only nominal realizations of the orbits of both (258656) 2002 ES_{76} and 2013 CC_{41}, and (ii) we included only gravitational perturbations from planets in our dynamical model. Both of these approximations are insufficient for a full analysis of our problem (see a similar discussion of the attempts to determine the origin of young asteroid clusters/families and pairs in Nesvorný & Vokrouhlický 2006, or Vokrouhlický & Nesvorný 2008).

First, the nominal orbital solution represents the best-fit of the available astrometric data. The inevitable uncertainties of the latter implies the uncertainty of the orbital fit itself. Well-behaved orbital solutions are represented by fixed confidence-level regions in the 6D orbital space, using an ellipsoidal geometry, mathematically expressed by elements organized in the covariance matrix. Each orbit starting in a high confidence-level zone ($\geq$80–90 per cent, say) is statistically equivalent to the best-fitting solution. Whilst initially very compact, these different solutions typically diverge with time. We thus need to consider in our simulation not only the best-fitting orbits, but also a sample of those starting from the high-confidence zone. We call these 'geometrical clones'.

The second issue that needs to be considered is the validity of the dynamical model used. The long-term dynamics of small objects are known to be subject to perturbations due to the thermal acceleration known as the Yarkovsky effect (e.g. Bottke et al. 2006; Vokrouhlický et al. 2015). Nominally, within the Trojan population, objects are only minimally affected by the Yarkovsky effect (Wang & Hou 2017; Hellmich et al. 2019), which has the greatest influence at smaller sizes. However, the two components in the (258656) 2002 ES_{76}–

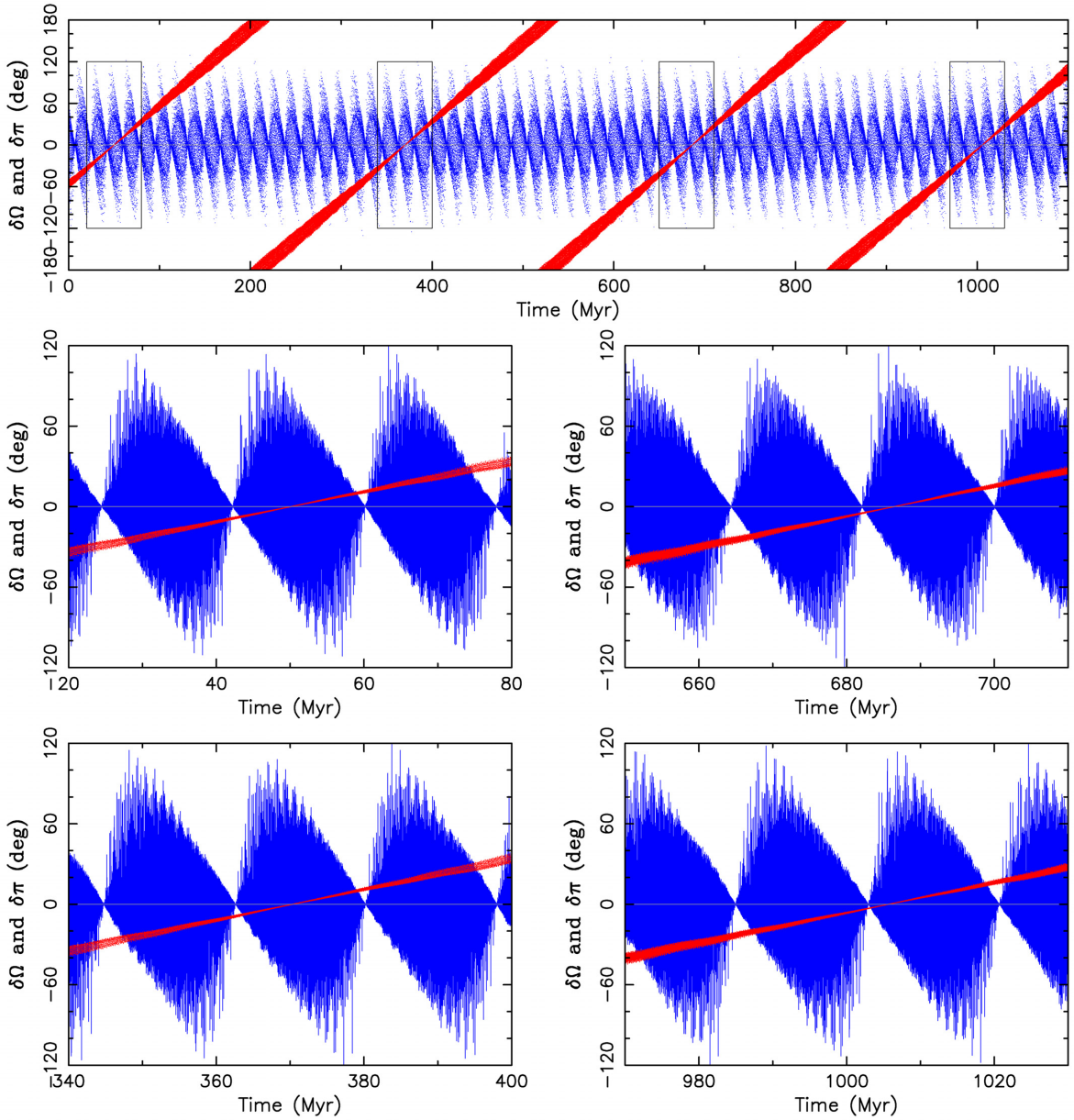

Figure 8. The long-term behaviour of the difference in osculating nodal and perihelion longitudes $\delta\Omega$ (red) and $\delta\varpi$ (blue) for the nominal orbits of (258656) 2002 ES_{76} and 2013 CC_{41}. The top panel shows the results from a backward integration in time to 1200 Myr. The four panels below show a zoom around the configurations where $\delta\Omega$ becomes small, also indicated by the black rectangles in the top panel. As inferred from data in Fig. 7, the first such situation occurs $\simeq$50 Myr in the past, and repeats with a period of $\simeq$320 Myr. The configuration of the nominal orbit becomes closest to true convergence at $\simeq$680 Myr and $\simeq$1010 Myr in the past (right middle and bottom panels).

2013 CC_{41} couple are well within this size range, and so it is warranted to see what dynamical effects might be produced by Yarkovsky accelerations. Since none of the parameters needed for evaluation of the thermal accelerations, such as the rotation state, the surface thermal inertia, and the bulk density, are known for either (258656) 2002 ES_{76} or 2013 CC_{41}, we need to consider a suite of potential orbit histories, each generated by numerical integration of test particles experiencing a range of physically plausible thermal accelerations. These will be called the Yarkovsky clones. We also note that the effect of thermal accelerations was included in `swift_rmvs4` using the same method as described in Vokrouhlický & Nesvorný (2008).

3.3 Clone sets

We conducted two sets of numerical simulations, one considering only the geometrical clones (Section 3.3.1), and the other considering only the Yarkovsky clones (Section 3.3.2) of (258656) 2002 ES_{76} and 2013 CC_{41}. In each simulation set, we include the nominal orbit of the objects, complemented by a set of 20 clones. We ran a backward integration of all orbits for 1.5 Gyr with an integration time-step of 3 d. Every 500 yr, we evaluated the differences between the osculating orbital elements of the 21 realizations of (258656) 2002 ES_{76} with each of those of 2013 CC_{41}, and searched for the possibility of a convergent configuration. To quantify the latter, we

used two conditions. First, as in Nesvorný & Vokrouhlický (2006), we evaluated the target function

$$\delta V = na\sqrt{(\sin I\,\delta\Omega)^2 + 0.5\,(e\,\delta\varpi)^2}, \quad (3)$$

where (n, a, e, I) are the arithmetically mean values of the mean motion, semimajor axis, eccentricity, and inclination of the two considered clones, and $\delta\Omega$ and $\delta\varpi$ are the differences between the osculating longitude of the ascending node and perihelion for the two clones, respectively. This way, δV has the dimension of velocity, and is constructed to provide, in a statistically mean sense, the necessary velocity perturbation required for a transfer between the secular angles of the two orbits. However, the analysis of the results presented in Fig. 8 has shown that even a configuration with potential $\delta\Omega \simeq 0$ and $\delta\varpi \simeq 0$, and therefore $\delta V \simeq 0$, is not enough to guarantee a satisfactory orbital convergence, provided that δe and δI are simultaneously large. For that reason, we admit as a potentially convergent configuration a case where the orbits of the two clones satisfy

(i) $\delta V \leq V_{\rm lim}$, where $V_{\rm lim}$ is some small value, we use typically 1–3 m s^{-1}, and

(ii) $\delta e \leq e_{\rm lim}$ and $\delta I \leq I_{\rm lim}$, where again we use suitably small values of $e_{\rm lim} \simeq 5 \times 10^{-4}$ and $I_{\rm lim} \simeq 0.1^\circ$ namely differences in the corresponding proper elements of (258656) 2002 ES$_{76}$ and 2013 CC$_{41}$.

We output information about these potentially converging configurations for further analysis. In the next two sections, we comment on the results of our numerical experiments that use geometrical (Section 3.3.1) and Yarkovsky clones (Section 3.3.2) separately.

3.3.1 Geometric clones

Information about the orbit determination, needed for a construction of the geometrical clones, was taken from the AstDyS data base. The orbits of both (258656) 2002 ES$_{76}$ and 2013 CC$_{41}$ are rather well constrained, reflecting numerous astrometric observations. Even the poorer of the two, 2013 CC$_{41}$, was observed over seven oppositions, leading to a fractional accuracy of $\simeq 10^{-7}$ in the semimajor axis, a, and the Cartesian components of the non-singular elements, z and ζ. Only the mean longitude, λ, has a slightly worse accuracy, namely $\simeq 2 \times 10^{-5}$ deg. These are the characteristic differences between the six orbital osculating elements $\mathbf{E} = (a, z, \zeta, \lambda)$ of the clones in $\simeq$68 per cent confidence zone and the best-fitting solution $\mathbf{E}_\star$. The solution is given at the initial epoch MJD58800. Complete information about the parameters of the 6D confidence zone ellipsoid in the space of elements $\mathbf{E}$ is given by the covariance and normal matrices, also provided at the AstDyS website. Denoting Σ the normal matrix, we may construct the initial orbital elements $\mathbf{E}$ of the geometric clones using

$$\mathbf{E} = \mathbf{T}^{\rm T}\xi + \mathbf{E}_\star, \quad (4)$$

where ξ is a 6D vector whose components are random deviates of normal distribution (with variance equal to unity), and the matrix $\mathbf{T}$ satisfies $\mathbf{T}^{\rm T}\mathbf{T} = \Sigma$ (e.g. Milani & Gronchi 2010); $\mathbf{T}$ is obtained using the Cholesky decomposition method. As mentioned above, we constructed 20 geometric clones of both (258656) 2002 ES$_{76}$ and 2013 CC$_{41}$ at the initial epoch of our simulation.

The bottom panel of Fig. 9 shows the maximum nodal difference between the clones of (258656) 2002 ES$_{76}$ and its nominal orbit. Tiny differences between the orbital parameters imply that the s frequency of the clone orbits is not exactly the same as that of the nominal orbit. However, the stability of this orbital zone ensures that the configuration of the clone orbits does not evolve, and thus initially the nodal divergence is basically linear in time. Only beyond about 0.5 Gyr does the divergence become stronger than linear. This is an expression of a very weak instability that manifests itself in the behaviour of the secular angle solely Gyr time-scales. The formal Lyapunov time-scale of the orbits of both (258656) 2002 ES$_{76}$ and 2013 CC$_{41}$ is only $\simeq$20 Myr (see the AstDyS data base). This implies that a divergence in λ is dominant, whilst the divergence in the secular angles is slower, as shown in Fig. 9. At 1 Gyr, the nodal longitudes of clones of (258656) 2002 ES$_{76}$ are thus spread over a $\simeq 2^\circ$ range. A similar, and potentially slightly larger, effect is seen among the clones of 2013 CC$_{41}$, principally due to their larger differences at the initial epoch. This divergence may overcome the difficulties we experienced in attempting to find an epoch at which the nominal orbits achieve a converging configuration. For instance, in the bottom right-hand panel of Fig. 8, we note that the nodal difference of the nominal orbits misses the epoch at which the difference of pericentres basically shrinks to zero by about 3° at $\simeq$1 Gyr. This may be compensated for if the orbits of suitable clones are used, instead of the nominal orbits.

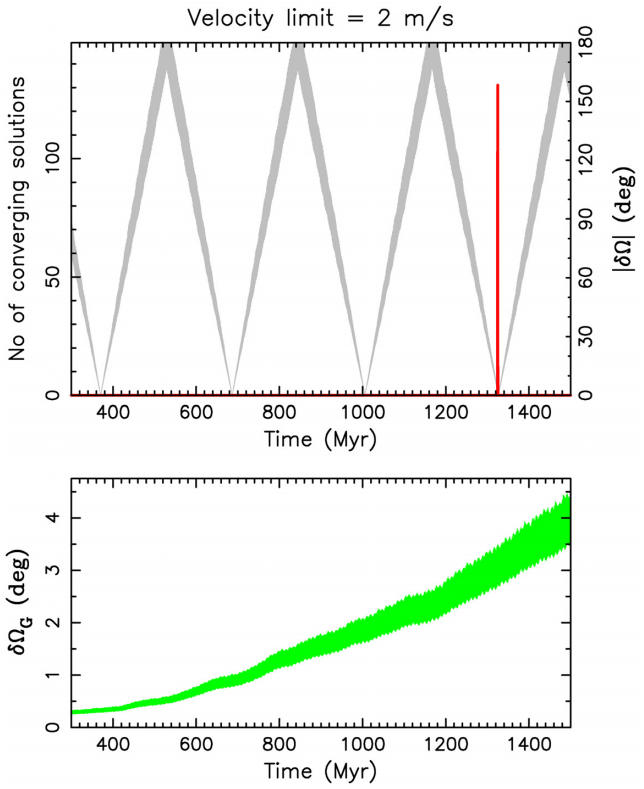

Figure 9. The statistical distribution of convergent solutions for geometric clones of (258656) 2002 ES$_{76}$ and 2013 CC$_{41}$ from simulations of the nominal orbits of the two objects, plus 20 clones each, using the velocity cutoff $\delta V \leq 2$ m s^{-1}, and eccentricity and inclination limits discussed in the text. Abscissa is time to the past starting from 300 Mya (there are no earlier solutions).The left ordinate in the upper two panels gives the number of recorded solutions in 50 kyr bins (red histogram). The grey line gives $|\delta\Omega|$ of the nominal orbits of (258656) 2002 ES$_{76}$'s and 2013 CC$_{41}$ (see the right ordinate and the red line on Fig. 8), aiming to aid interpretation of the results. The green line in the bottom panel shows the maximum difference in the longitude of the ascending node between the clones of (258656) 2002 ES$_{76}$ and the longitude of ascending node of its nominal orbit; up to about 200 Myr this trend is nearly linear, but becomes more complicated beyond this epoch due to very weak orbital chaos.

Obviously, a satisfactorily large nodal spread of the clone orbits must be attained.

The top panel of Fig. 9 shows the statistical distribution of the converging geometric clones of the two Trojans, organized in 50 kyr wide bins. Obviously, the rather small number of clones in our test run does not allow us to probe the convergence properties in great detail. For that reason, and with the rather tight limit $\delta V \leq 2\,\mathrm{m\,s^{-1}}$ chosen, the possible solutions cluster only near the $\simeq$1325 Myr epoch, though we note that, if a looser criterion $\delta V \leq 4\,\mathrm{m\,s^{-1}}$ was chosen, more solutions would also exist at $\simeq$1003 Myr. Taken naively at a face value, we would conclude a possible origin of the (258656) 2002 ES_{76}–2013 CC_{41} couple at this time in the past, if the couple are not older than 1.5 Gyr, beyond which we did not continue our simulation. However, as is often in the case of a pair configuration which is not very young, the so far neglected thermal accelerations in the dynamical model can prove to be a source of considerable uncertainty.This is analysed in Section 3.3.2.

3.3.2 Yarkovsky clones

Our Yarkovsky clones all have the same initial conditions as the nominal orbit, but they differ in the magnitude of thermal accelerations used for their orbital propagation. As in Vokrouhlický & Nesvorný (2008), we approximate thermal accelerations using a simple transverse component with the magnitude inversely proportional to the square of the heliocentric distance. The magnitude of this acceleration is adjusted such that the resulting change in the semimajor axis da/dt matches predictions from the theoretical formulation of Yarkovsky effect (see also Farnocchia et al. 2013, where a classical formalism used in cometary dynamics was adopted). In order to estimate plausible da/dt values, we use a simple approach describing the diurnal Yarkovsky effect for a spherical body on a circular heliocentric orbit, presented in Vokrouhlický (1998). We use the following set of physical parameters: the surface thermal conductivity $K \simeq 0.01$–$0.03\,\mathrm{W\,m^{-1}\,K^{-1}}$, the surface thermal inertia $\Gamma \simeq 100$–200 [SI units] (for both see Delbó et al. 2015), the bulk density $\rho \simeq 1.5\,\mathrm{g\,cm^{-3}}$ (e.g. Carry 2012), rotation period $P \simeq 100$–500 h, and size $D \simeq 7$ km. The maximum semimajor axis drift rate at zero obliquity is then $(\mathrm{d}a/\mathrm{d}t)_{\max} \simeq (0.15 \pm 0.07) \times 10^{-4}$ au Myr^{-1}. Our choice of a slow rotation period is tied to the working assumption that (258656) 2002 ES_{76} and 2013 CC_{41} are indeed a real Trojan pair. We argue in Section 4.1 that the most plausible formation mechanism for such a pair is the destabilization of a Trojan binary. If this is indeed the case, then before their separation, the two components were most likely spin–orbit synchronized to periods of $\geq$100 h (e.g. Nesvorný et al. 2020). If, however, the formation mechanism of the pair was different, such as the YORP-driven fission of a parent object (see Section 4.2), the rotation periods P of (258656) 2002 ES_{76} and 2013 CC_{41} could well be as short as a few hours. In that case, $(\mathrm{d}a/\mathrm{d}t)_{\max}$ would be smaller by a factor of 3 to 5. Indeed, as a confirmation of our reasoning, we note that scaling the value of the detected Yarkovsky signal 19×10^{-4} au Myr^{-1} for the 500 m size near-Earth asteroid 101955 Bennu with $P \simeq 4.3$ h (e.g. Chesley et al. 2014), we would have $(\mathrm{d}a/\mathrm{d}t)_{\max} \simeq 0.06 \times 10^{-4}$ au Myr^{-1}. In our simulation, we consider only the case of long rotation periods, and fix $(\mathrm{d}a/\mathrm{d}t)_{\max} \simeq 0.15 \times 10^{-4}$ au Myr^{-1}. For each of the two Trojans, (258656) 2002 ES_{76} and 2013 CC_{41}, we consider the nominal orbit with da/dt = 0, and 20 Yarkovsky clones. In both cases, 10 clones have positive da/dt and 10 clones have negative da/dt. Additionally, because in the case of the diurnal variant of the Yarkovsky effect da/d$t \propto \cos\gamma$, where γ is the spin axis obliquity, the positive/negative close da/dt values uniformly sample the interval 0 to $(\mathrm{d}a/\mathrm{d}t)_{\max}$, resp. $-(\mathrm{d}a/\mathrm{d}t)_{\max}$ to 0.

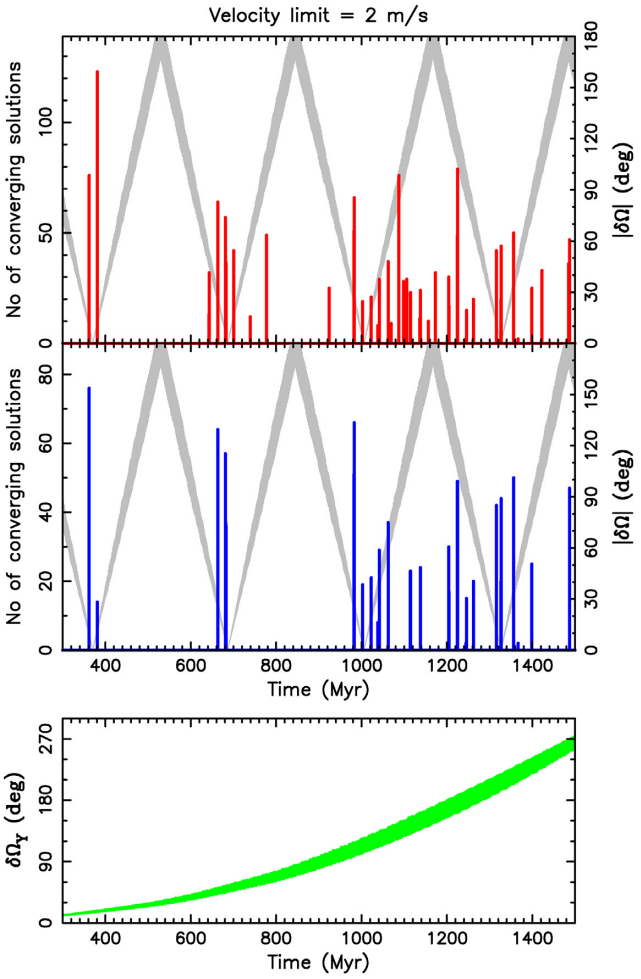

Figure 10. The statistical distribution of convergent solutions for the Yarkovsky clones (nominal orbits plus 20 clones each) of (258656) 2002 ES_{76} and 2013 CC_{41}, using the velocity cutoff $\delta V \leq 2\,\mathrm{m\,s^{-1}}$, and eccentricity and inclination limits discussed in the text. Abscissa is time to the past starting from 300 Mya (there are no earlier solutions). The left ordinate in the upper two panels gives the number of recorded solutions in 50 kyr bins. The top panel (red histogram) gives the number of solutions for all possible combinations of clones. The middle panel (blue histogram) for the case when only clones with the same sign of da/dt were compared. The grey line gives $|\delta\Omega|$ of the (258656) 2002 ES_{76}'s and 2013 CC_{41}'s nominal orbits (see the right ordinate and the red line on Fig. 8), aiming to aid interpretation of the results. The green line in the bottom panel shows the difference in the longitude of ascending node between the Yarkovsky clone with maximum positive drift rate $(\mathrm{d}a/\mathrm{d}t)_{\max}$ and the nominal orbit of (258656) 2002 ES_{76}.

Fig. 10 shows the results from our Yarkovsky clone simulations. In contrast to the simulations where only the geometrical clones were used (Fig. 9), there are many more convergent solutions, starting from 360 Mya. The reason is illustrated in the bottom panel of Fig. 10, which shows the divergence of the osculating longitude of the ascending node between the nominal orbit (no Yarkovsky effect) and the clone with the maximum positive drift-rate $(\mathrm{d}a/\mathrm{d}t)_{\max}$ of (258656) 2002 ES_{76}. Clones with smaller da/dt values have nodal differences smaller than the signal seen in Fig. 10, proportionally to their cos γ value.

The nodal differences between various clones are now much larger, reaching the maximum possible value of 360° after at ≃1.1 Gya. The nodal difference to the nominal orbit of the clone with the maximum negative drift-rate value is about the same but negative. This is because $\delta\Omega$ now propagates nearly quadratically in time as opposed to the quasi-linear trend for the geometrical clones. Such a quadratic trend in node propagation is characteristic of Yarkovsky studies of asteroids (e.g. Vokrouhlický & Nesvorný 2008). In that case, the phenomenon was easily associated with the principal dynamical perturbation produced by the Yarkovsky effect, namely the secular drift in semimajor axis. As a result, the semimajor axis dependence of the s frequency produces, after a straightforward integration, a quadratic-in-time drift of the node. In our case of Jovian Trojans, the effects are slightly subtler. This is because, in spite of a permanent transverse perturbing acceleration in orbits of the clones, their semimajor axis does not show any constant drift in time due to the resonant locking inherent to their presence in the Trojan population. However, other elements – eccentricity and inclination – do display such a secular drift, as previously found in Wang & Hou (2017) and Hellmich et al. (2019). As the s frequency is also dependent on these values, it still displays a linear change as a function of time, explaining the quadratic effect in node seen in the Fig. 10.

Returning to the pattern in the distribution of converging solutions seen in Fig. 10, we note their clustering near epochs when $\delta\Omega$ of the (258656) 2002 ES_{76} and 2013 CC_{41} nominal orbits has been found to reach zero (the grey line in the top panels). This is to be expected, since the nodal difference exhibits the most stable evolution in time. Therefore, when nominal orbits of the two Trojans have large $\delta\Omega$ values, the clones will also follow the same pattern. This conclusion will, however, weaken further into the past because of the clone nodal divergence discussed above. As a result, beyond ∼ 1Gyr into the past, the solution distribution spreads more in time. This is because specific clone combinations may now satisfy more easily our convergence conditions. Additionally, convergent solutions cluster in peaks separated by about 19 Myr, rather than exhibiting a continuous distribution about the $\delta\Omega \simeq 0$ nodal conditions. This is due to the $\delta\varpi \simeq 0$ perihelion condition also facilitating the convergence criteria we adopted.

The middle panel in Fig. 10 shows the statistical distribution of the number of converging solutions for a subsample of cases in which clones of (258656) 2002 ES_{76} and 2013 CC_{41} both have the same sign of the associated da/dt drift. Translated using the diurnal Yarkovsky theory, this also implies that the two clones have the same sense of rotation: either both prograde, or both retrograde. The proposed formation mechanisms for this pair, namely a binary split or rotation fission, would both predict this property. There are obviously fewer solutions found, but the general pattern of their distribution is about the same as in the general case when all clones are taken into account.

Fig. 11 shows the conditions at convergence for two pairs of the Yarkovsky clones of (258656) 2002 ES_{76} and 2013 CC_{41}: the left-hand panels at the most recent possible cluster of solutions in the past (namely at ≃381.07 Mya), whilst the right-hand panel shows the cluster at an epoch which is more distant in the past by two cycles of the differential motion of their orbital nodes (namely at ≃1062.33 Mya). In general, the quality of the convergence is similar, including those solutions beyond 1 Gya. In both cases, the formal convergence of the secular angles is better than 0.004°.

When inserted into equation (3), the equivalent velocity difference is negligibly small $\delta V \leq 0.04\,\mathrm{m\,s^{-1}}$. At the convergence epoch, the osculating eccentricity values are also satisfactorily close to each other, namely $\delta e \simeq 7.5 \times 10^{-5}$. Using the Gauss equations (e.g. Nesvorný & Vokrouhlický 2006), we estimate that this tiny eccentricity difference corresponds to an orbital velocity change smaller than $1\,\mathrm{m\,s^{-1}}$ in a statistical sense. This change is actually smaller than the difference in proper eccentricity values of (258656) 2002 ES_{76} and 2013 CC_{41}. The inclination convergence turns out to be the most troublesome element of the simulation: the persisting differences of ≃0.085° statistically correspond to a velocity change of $\simeq 25\,\mathrm{m\,s^{-1}}$. Such a difference in the osculating values of inclinations corresponds to the difference of their proper values. In contrast, the acceptable true separation velocity of the objects should be a fraction of the escape velocity from the effective parent body. With its size of ≃9 km, the ideal condition of the separation in this pair would require a velocity difference of $\leq 4\,\mathrm{m\,s^{-1}}$. The inclination difference at converging solutions is therefore nearly an order of magnitude larger.

One possibility to explain this mismatch may be related to our approximation of the Yarkovsky effect. By representing it using the transverse acceleration only, the inclination is not perturbed. In fact, a complete model of the thermal accelerations may admit an out-of-plane component, provided that the obliquities of the components of the pair are not extreme (e.g. Vokrouhlický 1998). However, to fully use such a model, we would need to sample a multiparametric space of possible spin orientations and physical parameters for Yarkovsky clones, an effort which is postponed to further studies.

An alternative dynamical mechanism, that has not been included in our simulations, consists of perturbations from the largest Trojans in the L_4 swarm. As an example, we consider the influence 624 Hektor, whose mass is estimated to be $\simeq 10^{17}$ kg (e.g. Carry 2012), about 10^{-4} of the mass of dwarf-planet 1 Ceres. Nesvorný et al. (2002b) found that, statistically, the mean perturbation of the orbital inclination produced by Ceres in the inner and middle parts of the Main belt is ≃1.5° in 4 Gyr. Assuming the effect scales with the square root of the perturber mass, we estimate that the approximate effect of Hektor on small L_4 Trojans would be ≃0.015° over 4 Gyr, in a statistical sense. Therefore, at least a part of the inclination mismatch reported above could well be due to the ongoing scattering influence of the most massive Trojans.

4 FORMATION OF THE TROJAN PAIR

We now briefly discuss possible formation processes for the (258656) 2002 ES_{76}–2013 CC_{41} pair. In principle, these mechanisms coincide with the suggestions outlined in Section 6 of Vokrouhlický & Nesvorný (2008). Building on that work, we will skip for now the possibility that these two Trojans are the two largest objects in a compact, collisionally born family. Given their comparable size, the collision required to form such a family must have been supercatastrophic, with many kilometre size fragments created and dominating the mass. Without information about them, it is hard to say anything more about the putative collision conditions, including the probability of such a collision actually having occurred.

4.1 Collisional dissociation of a synchronous binary

The first possible origin for the (258656) 2002 ES_{76}–2013 CC_{41} pair consists of a model, in which the two objects were formerly components in a binary system which underwent some kind of instability. We assume that the instability was not of a dynamical origin. Indeed, even if formed by gravitational collapse, the initial angular momentum of the binary would exceed that of a critically rotating single body of an equivalent mass by a factor of ≃(3–10) (Nesvorný et al. 2019). This is not sufficient to drive tidal evolution, whilst conserving angular momentum, to the stability

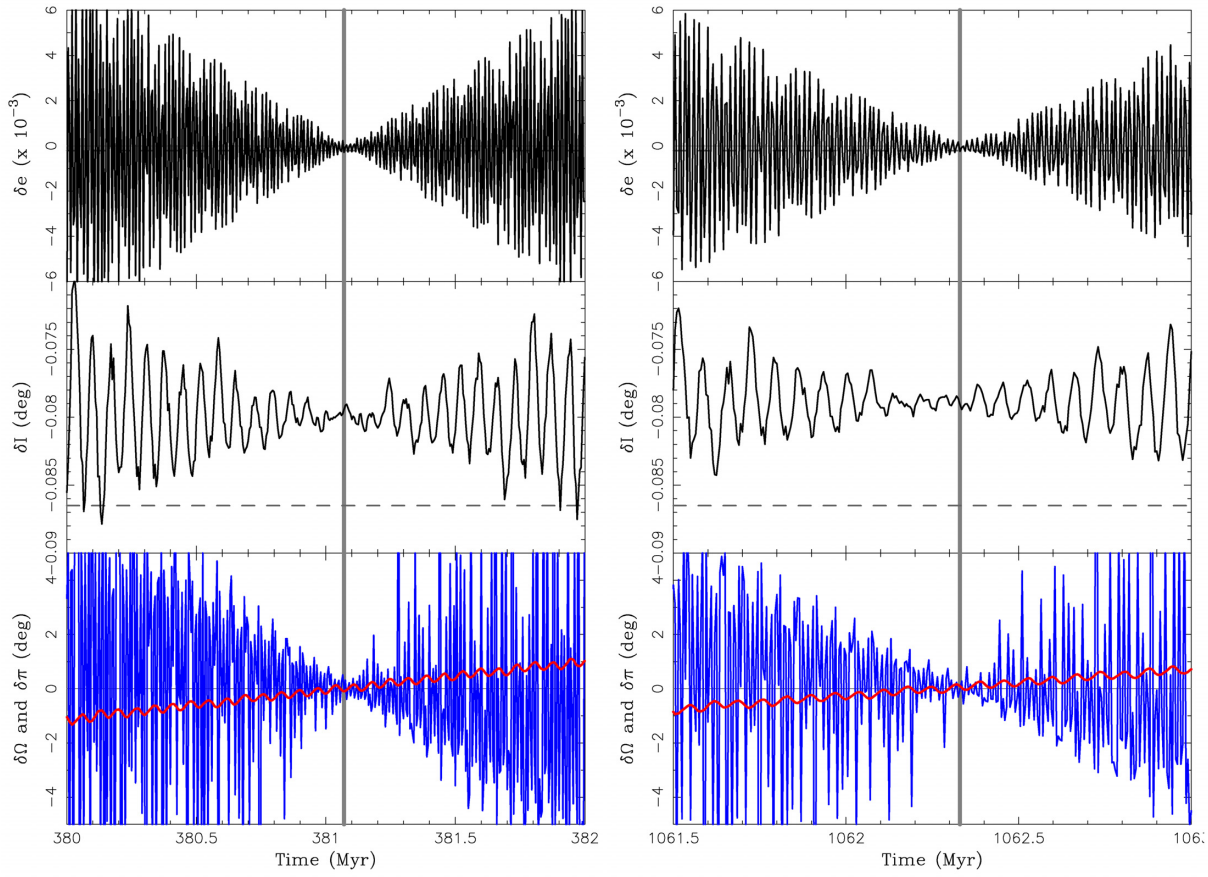

Figure 11. Two examples of converging solutions between Yarkovsky clones of (258656) 2002 ES_{76} and 2013 CC_{41}: left-hand panels at ≃381.07 Mya, right-hand panels at ≃1062.33 Mya (grey vertical lines show the nominal convergence epochs). Each of the panels shows the differences between the osculating orbital elements of the clones: eccentricity (top), inclination (middle), and longitude of node (red) and perihelion (blue; bottom). The secular angles Ω and ϖ converge to better than 0.004°, corresponding to a negligible value of the target function $\delta V \leq 0.04\,\mathrm{m\,s^{-1}}$ (see equation 3). Differences in e and I are relatively larger, namely $\delta e \simeq 7.5 \times 10^{-5}$ and $\delta I \simeq 0.079°$ (left), resp. $\delta I \simeq 0.078°$ (right). The dashed horizontal lines show the differences between the respective proper elements of (258656) 2002 ES_{76} and 2013 CC_{41}. Note the ordinate of the middle panel (inclination) which is offset from zero.

limit at about half of the Hill sphere, even in the Trojan zone. The limiting configuration would require angular momentum at least twice as large. Additionally, time constraints may prevent evolution to such large separations within ≤4.5 Gyr. Therefore, the nature of the parent binary instability must be different. We assume instead that this instability was triggered by a gentle-enough impact on one of the components. We leave aside other possibilities, such as binary instability produced during a close three-body encounter with a massive Trojan (Agnor & Hamilton 2006; Nesvorný & Vokrouhlický 2019), for future investigations, once the mechanisms are better understood in the Jovian Trojan population.

Let us start the likelihood analysis of the formation of the (258656) 2002 ES_{76}–2013 CC_{41} pair via the subcritical impact dissociation of a previously existing synchronous binary with a very simple, order-of-magnitude estimate. Assume that the needed imparted velocity by the impact on to a ≃7 km size component in the binary is about $1\,\mathrm{m\,s^{-1}}$. Then, using the simple formulation in Nesvorný et al. (2011), a projectile of ≃0.53 km size is required. The characteristic impact velocity assumed was $V_{\mathrm{imp}} \simeq 4.6\,\mathrm{km\,s^{-1}}$ (Davis et al. 2002). The Trojan population contains very approximately $N \simeq 400\,000$ such objects (e.g. Emery et al. 2015; Wong & Brown 2015; and Fig. 12).

Using the mean impact probability $p_i \simeq 7 \times 10^{-18}\,\mathrm{km^{-2}\,yr^{-1}}$ (e.g. Davis et al. 2002), we can therefore estimate the order-of-magnitude likelihood that such an event would occur within a timeframe of T

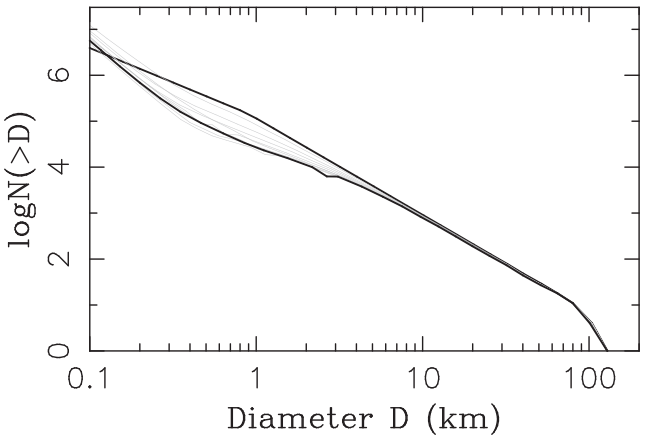

Figure 12. The effects of collisional grinding on the cumulative size distribution of Jovian Trojans. The upper bold line is the initial distribution. The lower bold line is the size distribution at $T = 4.5$ Gyr. The grey lines show the changing size distribution in 500 Myr intervals. The dip in the final distribution near $D = 0.5$ km is produced by the strength-to-gravity transition of the disruption law.

$\simeq 4.5$ Gyr, namely $p_i R^2 NT \simeq 0.15$ (here $R = 3.5$ km is the radius of the target body). This suggests that every such binary implanted to the Trojan population has a non-negligible (15 per cent) chance to be split via this process. Assuming that, initially, at least hundreds of binaries were captured intact to the Trojan population, a non-negligible number of Trojan pairs might have been created over the age of the Solar system. Obviously, in many cases, our ability to identify the pair produced in this manner is low, due to unsuitable locations in the Trojan orbital phase space. Nonetheless, this result suggest that sufficiently many such pairs could be produced that future study might well reveal several more.

We now substantiate this order-of-magnitude estimate using a more involved numerical simulation. As outlined above, the mutual orbit of a binary can be affected by small impacts on to its components. The binary may become unbound if the velocity change imparted by an impact exceeds binary's orbital speed $\sim$0.2–2 m s^{-1} for bodies with $D \simeq 7$ km (Petit & Mousis 2004).

We investigate this process with the previously developed collisional code (Morbidelli et al. 2009; Nesvorný et al. 2011). The code, known as `Boulder`, employs a statistical method to track the collisional fragmentation of planetesimal populations. A full description of the `Boulder` code, tests, and various applications can be found in Morbidelli et al. (2009), Levison et al. (2009), and Bottke et al. (2010). The binary module in `Boulder` accounts for small, non-disruptive impacts on binary components, and computes the binary orbit change depending on the linear momentum of impactors (see Nesvorný et al. 2011; Nesvorný & Vokrouhlický 2019).

We account for impacts over the life of the Solar system, 4.5 Gyr. The captured population of Jovian Trojans is assumed to be similar to the present population, for objects with large diameters. There are $\simeq$25 Trojans with $D > 100$ km. The population is assumed to follow a power-law profile below 100 km, with a cumulative index equal to -2.1 (Fig. 12). The intrinsic impact probability and impact velocity is the same as used for the order-of-magnitude estimate above. We adopt a standard disruption law for solid ice from Benz & Asphaug (1999). Fragments are generated according to the method described in Morbidelli et al. (2009). These rules are implemented in the `Boulder` code, which is then used to determine the collisional survival of Trojan binaries (e.g. Nesvorný et al. 2018).

Fig. 12 shows the evolution of the size distribution for the Jovian Trojans. The size distribution for $D > 10$ km remains unchanged over 4.5 Gyr, but below $D \simeq 5$ km the slope becomes shallower. This is consistent with Jovian Trojan observations that detect a shallower slope for $D \simeq 3$ km (e.g. Wong & Brown 2015). If this interpretation is correct, the slope should become steeper below approximately 500 m, for bodies that are too faint to be detected from the ground using the current generation of observatories. The dip in the size distribution is produced by the transition from strength-to-gravity dominated branches of the disruption law (e.g. Nesvorný et al. 2018).

We find that the survival chances of Trojan binaries are generally good, but drop significantly when the binary separation approaches 0.5 R_H (R_H being the Hill sphere of gravitational influence, see Fig. 13). This is expected because binaries with semimajor axis $a_B > 0.5\ R_H$ are dynamically unstable (e.g. Porter & Grundy 2012). For a characteristic separation of $a_B/(R_1 + R_2) \simeq 10-100$, where a_B is the binary semimajor axis and R_1 and R_2 are the binary component radii, consistent with the pair (258656) 2002 ES$_{76}$–2013 CC$_{41}$ ($R_1 + R_2 = 7.2$ km), which is quite common among equal-size binaries in the Edgeworth-Kuiper belt (e.g. Noll et al. 2020), the survival probability is 7–40 per cent. There is plenty of room in this parameter space for Trojan pair formation by this mechanism. Assuming that the pair (258656) 2002 ES$_{76}$–2013 CC$_{41}$ is an impact-dissolved binary, we find that there should be 0.08–0.7 surviving binaries for each pair such as (258656) 2002 ES$_{76}$–2013 CC$_{41}$. Given that the vast majority of Trojan pairs remain undetected (see the difficulties briefly outlined in Appendix B), the obvious implication is that there should also be several equal-size binaries among Jovian Trojans in this size range.

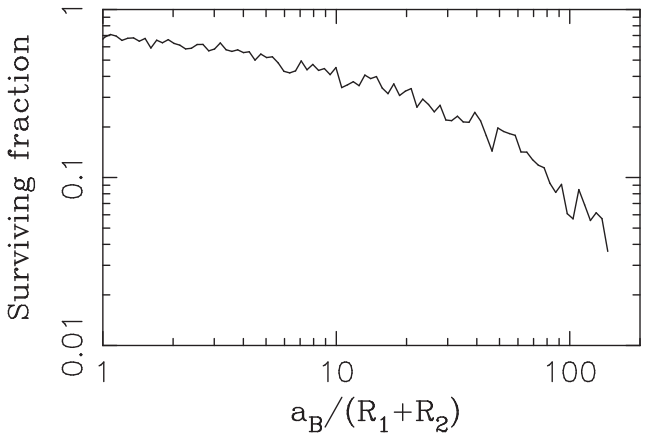

Figure 13. The survival probability of binaries with (258656) 2002 ES$_{76}$–2013 CC$_{41}$ components as a function of separation, here normalized to the sum of physical radii, $R_1 + R_2$. The survival probability decreases with separation because wide binaries have smaller orbital speeds and are easier to dissolve by a small impact. For reference, the Hill radius R_H of a binary with (258656) 2002 ES$_{76}$–2013 CC$_{41}$ components, corresponding to mass $\sim 5 \times 10^{17}$ g (for 1 g cm^{-3} density), is $R_H \simeq 3,400$ km, or nearly $a_B/(R_1 + R_2) = 500$.

4.2 Rotational fission of a parent object

An alternative formation mechanism that could explain the observed properties of the (258656) 2002 ES$_{76}$–2013 CC$_{41}$ pair is that they might be the result of the rotational fission of their common parent object (this is indeed the favourite mechanism for asteroid pair formation in the main belt; e.g. Pravec et al. 2010). The most probable driving process for such a fission event is the Yarkovsky-O'Keefe-Radzievski-Paddack (YORP) effect, a radiative torque resulting from the combination of reflected and thermally emitted radiation by the surface (being thus a complementary phenomenon to the Yarkovsky effect; e.g. Bottke et al. 2006; Vokrouhlický et al. 2015). The YORP effect is able to constantly accelerate an asteroid's rotation up to speeds that meet the requisite conditions to cause the object to fission. The rotation frequency change $\dot{\omega}$ satisfies general scaling properties, such that $\dot{\omega} \propto 1/[\rho\,(aD)^2]$, where ρ is the bulk density, a the orbital semimajor axis, and D the size. However, the problematic part of the YORP effect, unlike the Yarkovsky effect, is its large sensitivity to details of the surface roughness. For that reason it is troublesome to determine the exact value of the strength of the YORP effect for a given object, and we must satisfy ourselves with an order-of-magnitude estimate in our case.

If we were to determine the doubling time-scale $\tau_{YORP} = \omega/\dot{\omega}$ (sometimes also the YORP cycle time-scale; e.g. Rubincam 2000), it would be reasonable to use the YORP detection of the small near-Earth asteroid (101955) Bennu as a template, as we did above for the Yarkovsky effect in Section 3.3.2. (101955) Bennu has $\tau_{YORP} \simeq 1.5$ Myr (e.g. Hergenrother et al. 2019). Adopting plainly the scaling $\tau_{YORP} \propto \rho\,(aD)^2/P$ (with P being the rotation period), we obtain $\tau_{YORP} \simeq 11$ Gyr for a $D \simeq 9$ km Trojan, the estimated size of a putative

parent object of the (258656) 2002 ES_{76}–2013 CC_{41} pair. Note that τ_{YORP} provides an estimate of a time-scale for doubling ω, as an example changing rotation period from 5 to 2.5 h, an approximate fission limit for a large internal strength Trojan model. Another $\tau_{YORP}/2 \simeq 5.5$ Gyr time would be needed if the initial rotation period of the parent object was 10 h. This shorter time-scale would also be an appropriate estimate to reach the fission limit at a longer period of $\simeq$5 h when the internal strength and bulk densities are low (e.g. French et al. 2015; Szabó et al. 2017).

If, however, we were to consider the results from numerical simulations of the YORP effect for a large statistical sample of Gaussian-sphere shapes Čapek & Vokrouhlický (2004), which obtained $\tau_{YORP} \simeq 15$ Myr for a typical main belt S-type asteroid of a 2 km size, we would have $\tau_{YORP} \simeq 1.5$ Gyr for changing the parent object period from 5 to 2.5 h. Whilst these results are known to typically overestimate the strength of the YORP effect by a factor of 3–5, when compared to detections of the YORP effect for small near-Earth asteroids, we none the less get a time-scale shorter by a factor 2 to 3 than for the Bennu case. The takeaway message is that the estimate of the YORP doubling time-scale prior the fission of the putative parent object of the (258656) 2002 ES_{76} and 2013 CC_{41} pair is very uncertain, with values ranging possibly from 2 Gyr to some 12 Gyr.

Taken at a face value, the smaller values in this interval are plausible as an explanation for the origin of the pair when compared to the lifetime of the Solar system. It may not be surprising to find that some $D \simeq 9$ km Jupiter Trojan objects undergo a rotational fission during their lifetime. However, a more detailed inspection of the (258656) 2002 ES_{76} and 2013 CC_{41} parameters speaks against this possibility. First, we note that the known rotation periods of Jovian Trojans rarely have values smaller than 8–10 h (e.g. French et al. 2015; Ryan, Sharkey & Woodward 2017; Szabó et al. 2017), which suggests in turn that more than one τ_{YORP} time-scale would be needed to reach fission from a typical initial rotation state (though, admittedly, these known data concern larger objects). More importantly, though, we note that the absolute magnitude difference of (258656) 2002 ES_{76} and 2013 CC_{41} is $\simeq$(0.2–0.3), depending on the data base used. This implies that the two objects are nearly of the same size. Pravec et al. (2010) argued that the typical conditions of fission mechanics require at least 1 magnitude difference between the two components in pair. This is because some degree of size disparity is needed to make the two components separate on to distinct heliocentric orbits. Whilst exceptions have been found to this guideline (see e.g. Pravec et al. 2019), the majority of the known asteroid pairs, more than 90 per cent, satisfy this condition of having a large enough magnitude disparity. The components in the (258656) 2002 ES_{76}–2013 CC_{41} pair violate this rule and would require special conditions for their separation to feasibly be the result of rotational fission.

5 CONCLUSIONS

In this work, we identified the first potential dynamical pair in the Jovian Trojan population. In particular, we analysed the distribution of Trojans in their proper orbital element space. Using information about the local density of objects, we also assessed the statistical significance of the proximity of potential couples. This procedure lead us to select a pair of bodies, (258656) 2002 ES_{76} and 2013 CC_{41}, in the L4 swarm as a potential candidate pair. Interestingly, this suggested pair is located very close to the L4 Lagrange point, with low proper elements, semimajor axis (da_P), eccentricity e_P, and sine of inclination ($\sin I_P$) values. Finally, as part of our effort, we developed an up-to-date, highly accurate set of proper elements for the all Jovian Trojans, which we have made publicly available (Appendix A).

In order to further investigate the selected pair, we ran a series of n-body simulations, which were used to look for past convergences in the osculating nodal ($\delta\varpi$) and perihelion longitude ($\delta\Omega$) value for the two objects, whilst ensuring that, at the time of such convergences the differences in the osculating eccentricity and inclination were also sufficiently small. Our simulations included both geometric clones, created from the uncertainties in the orbital elements of the bodies, and Yarkovsky clones, based on the estimated thermal accelerations that the two objects could experience, for a variety of realistic rotation rates. As a result, we obtained a statistical set of convergences, finding a larger pool of possibilities once the Yarkovsky clones were included. Our results reveal that the pair is at least $\simeq$360 Myr old, but are compatible with the age being significantly older, potentially in the Gyr time-scale. By finding such possible convergences, we increase the confidence that the (258656) 2002 ES_{76}–2013 CC_{41} couple is a legitimate pair.

We then considered the mechanisms by which the (258656) 2002 ES_{76}–2013 CC_{41} pair could have formed (compared with Vokrouhlický & Nesvorný 2008). The pair is not associated with any known collisional family, and as such we do not favour the possibility of the pair having been formed as a result of a catastrophic impact on a putative parent body. The pair might have been formed through the rotational fission of their parent Trojan, since, for certain initial conditions, the time-scale for such an object to be spun-up by the YORP effect to the point that it undergoes fission could be somewhat shorter than the age of the Solar system. However, this pair consists of two nearly equal-sized components, whilst the vast majority of observed pairs formed by rotational fission have a size ratio of at least 1.5 (see Pravec et al. 2010, 2019). For that reason, we consider that the pair most likely formed as a result of the dissociation of an equal-size binary. We can confirm that such a scenario is indeed feasible using an estimation of the binary survival rate in the size range of the (258656) 2002 ES_{76}–2013 CC_{41} pair, $D \simeq 7$ km, over 4.5 Gyr, after implantation to the Trojan population early in Solar system's history. Statistically, this indicates that there should be many such pairs within the Trojan population in this 5–10 km size range. As the Rubin Observatory's Legacy Survey of Space and Time (LSST) comes online, it is expected to discover many Jovian Trojans in this size range (e.g. Schwamb et al. 2018). As new Trojans are discovered, our results suggest that further pairs should be revealed.

The (258656) 2002 ES_{76}–2013 CC_{41} pair provides an interesting clue to the past history of the Jovian Trojans, and the Solar system as a whole. So far, we know little beyond their dynamical properties and size estimations. In particular, light-curve analysis could assist in constraining the formation mechanism, as this would provide an estimate of the rotational periods of the two objects. Due to their small size, and dark albedo, the objects have relatively low apparent magnitudes, at best $\simeq$20.5 magnitude in visible band. In order to further characterize these objects, observations using large Earth-based facilities, such as the SUBARU (Kashikawa et al. 2002) or Keck (Oke et al. 1995) telescopes, will be required. These objects would also benefit from future observations using the *James Web* (*JWST*; Rivkin et al. 2016) and *Nancy Grace Roman Space* Telescopes (RST, formerly known as *WFIRST*; Holler et al. 2018). Time on these telescopes is competitive, but we recommend proposals for observations of (258656) 2002 ES_{76} and 2013 CC_{41} be selected to further extend our understanding of this interesting pair of Trojans.

ACKNOWLEDGEMENTS

TRH was supported by the Australian Government Research Training Program Scholarship. The work of DV and MB was partially supported by the Czech Science Foundation (grant 18-06083S). This research has made use of NASA Astrophysics Data System Bibliographic Services. We thank Dr. Romina Di Sisto for their valuable review of this manuscript.

We dedicate this paper to the memory of Andrea Milani and Paolo Farinella, who were the first to propose the idea of a genetically connected pair of objects in the Jovian Trojan population (Milani 1993).

DATA AVAILABILITY

The data base of Jovian Trojan proper elements is accessible at https://sirrah.troja.mff.cuni.cz/~mira/mp/trojans_hildas/, and is available for community use. See Appendix A for details.

REFERENCES

Agnor C. B., Hamilton D. P., 2006, Nature, 441, 192
Beaugé C., Roig F., 2001, Icarus, 153, 391
Benjoya P., Zappalà V., 2002, in Bottke W. F., Cellino A., Paolicchi P., Binzel R. P., eds, Asteroids III. University of Arizona Press, Tuckson, p. 613
Benz W., Asphaug E., 1999, Icarus, 142, 5
Bottke W. F., Vokrouhlický D., Rubincam D. P., Nesvorný D., 2006, Annu. Rev. Earth Planet. Sci., 34, 157
Bottke W. F., Nesvorný D., Vokrouhlický D., Morbidelli A., 2010, AJ, 139, 994
Brož M., Rozehnal J., 2011, MNRAS, 414, 565
Buie M. W. et al., 2015, AJ, 149, 113
Carry B., 2012, Planet. Space Sci., 73, 98
Chesley S. R. et al., 2014, Icarus, 235, 5
Davis A. B., Scheeres D. J., 2020, Icarus, 341, 113439
Davis D. R., Durda D. D., Marzari F., Campo Bagatin A., Gil-Hutton R., 2002, in Bottke W. F., Cellino A., Paolicchi P., Binzel R. P., eds, Asteroids III. University of Arizona Press, Tuckson, p. 545
Delbó M., Mueller M., Emery J. P., Rozitis B., Capria M. T., 2015, in Michel P., DeMeo F. E., Bottke W. F., eds, Asteroids IV. University of Arizona Press, Tuckson, p. 107
Di Sisto R. P., Ramos X. S., Beaugé C., 2014, Icarus, 243, 287
Di Sisto R. P., Ramos X. S., Gallardo T., 2019, Icarus, 319, 828
Emery J. P., Marzari F., Morbidelli A., French L. M., Grav T., 2015, in Michel P., DeMeo F. E., Bottke W. F., eds, Asteroids IV. University of Arizona Press, Tuckson, p. 203
Farnocchia D., Chesley S. R., Vokrouhlický D., Milani A., Spoto F., Bottke W. F., 2013, Icarus, 224, 1
French L. M., Stephens R. D., Coley D., Wasserman L. H., Sieben J., 2015, Icarus, 254, 1
Grav T. et al., 2011, ApJ, 742, 40
Grav T., Mainzer A. K., Bauer J. M., Masiero J. R., Nugent C. R., 2012, ApJ, 759, 49
Hellmich S., Mottola S., Hahn G., Kührt E., de Niem D., 2019, A&A, 630, A148
Hergenrother C. W. et al., 2019, Nat. Commun., 10, 1291
Holler B. J., Milam S. N., Bauer J. M., Alcock C., Bannister M. T., Bjoraker G. L., 2018, J. Astron. Telesc. Instrum. Syst., 4, 1
Holt T. R. et al., 2020, MNRAS, 495, 4085
Horner J., Müller T. G., Lykawka P. S., 2012, MNRAS, 423, 2587
Kashikawa N. et al., 2002, PASJ, 54, 819
Lagrange J.-L., 1772, Essai sur le Problème des Trois Corps, Prix de l'Académie Royale des Sciences de Paris printed in 1868, Œuvres de Lagrange, Tome VI. Gauthier-Villars, Paris, France, p. 229
Laskar J., Robutel P., 2001, Celest. Mech. Dyn. Astron., 80, 39
Levison H. F., Duncan M. J., 1994, Icarus, 108, 18
Levison H. F., Shoemaker E. M., Shoemaker C. S., 1997, Nature, 385, 42
Levison H. F., Bottke W. F., Gounelle M., Morbidelli A., Nesvorný D., Tsiganis K., 2009, Nature, 460, 364
Levison H. F., Olkin C. B., Noll K., Marchi S., Lucy Team, 2017, in Lunar Planet. Sci. Conf, p. 2025, http://adsabs.harvard.edu/abs/2017LPI....48.2025L
Marchis F. et al., 2006, Nature, 439, 565
Margot J.-L., Pravec P., Taylor P., Carry B., Jacobson S., 2015a, in Michel P., DeMeo F. E., Bottke W. F., eds, Asteroids IV. University of Arizona Press, Tuckson, p. 355
Margot J.-L., Pravec P., Taylor P., Carry B., Jacobson S., 2015b, in Michel P., DeMeo F.E., Bottke W.F., eds, Asteroids IV. University of Arizona Press, Tuckson, p. 355
Milani A., 1993, Celest. Mech. Dyn. Astron., 57, 59
Milani A., Gronchi G. F., 2010, Theory of Orbital Determination. Cambridge University Press, Cambridge
Morbidelli A., Bottke W. F., Nesvorný D., Levison H. F., 2009, Icarus, 204, 558
Moskovitz N. A. et al., 2019, Icarus, 333, 165
Nesvorný D., 2018, Annu. Rev. Astron. Astrophys., 56, 137
Nesvorný D., Vokrouhlický D., 2006, AJ, 132, 1950
Nesvorný D., Vokrouhlický D., 2019, Icarus, 331, 49
Nesvorný D., Thomas F., Ferraz-Mello S., Morbidelli A., 2002a, Celest. Mech. Dyn. Astron., 82, 323
Nesvorný D., Morbidelli A., Vokrouhlický D., Bottke W. F., Brož M., 2002b, Icarus, 157, 155
Nesvorný D., Vokrouhlický D., Bottke W. F., 2006, Science, 312, 1490
Nesvorný D., Vokrouhlický D., Bottke W. F., Noll K., Levison H. F., 2011, AJ, 141, 159
Nesvorný D., Brož M., Carruba V., 2015, in Michel P., DeMeo F. E., Bottke W. F., eds, Asteroids IV. University of Arizona Press, Tuckson, p. 297
Nesvorný D., Vokrouhlický D., Bottke W. F., Levison H. F., 2018, Nat. Astron., 2, 878
Nesvorný D., Li R., Youdin A. N., Simon J. B., Grundy W. M., 2019, Nat. Astron., 3, 808
Nesvorný D., Vokrouhlický D., Bottke W. F., Levison H. F., Grundy W. M., 2020, ApJ, 893, L16
Noll K., Grundy W. M., Nesvorný D., Thirouin A., 2020, in Prialnik D., Barucci M. A., Young L., eds, The Trans-Neptunian Solar System. University of Arizona Press, Tuckson, p. 201
Oke J. B. et al., 1995, Publ. Astron. Soc. Pacific, 107, 375
Petit J. M., Mousis O., 2004, Icarus, 168, 409
Porter S. B., Grundy W. M., 2012, Icarus, 220, 947
Pravec P. et al., 2010, Nature, 466, 1085
Pravec P. et al., 2019, Icarus, 333, 429
Pravec P., Harris A. W., 2007, Icarus, 190, 250
Pravec P., Vokrouhlický D., 2009, Icarus, 204, 580
Quinn T. R., Tremaine S., Duncan M., 1991, AJ, 101, 2287
Rivkin A. S., Marchis F., Stansberry J. A., Takir D., Thomas C., 2016, Publ. Astron. Soc. Pacific, 128, 018003
Robutel P., Gabern F., 2006, MNRAS, 372, 1463
Rozehnal J., Brož M., Nesvorný D., Durda D. D., Walsh K., Richardson D. C., Asphaug E., 2016, MNRAS, 462, 2319
Rożek A., Breiter S., Jopek T. J., 2011, MNRAS, 412, 987
Rubincam D. P., 2000, Icarus, 148, 2
Ryan E. L., Sharkey B. N. L., Woodward C. E., 2017, AJ, 153, 116
Schwamb M. E. et al., 2018, preprint (arXiv:1802.01783)
Szabó G. M. et al., 2017, A&A, 599, A44
Tsiganis K., Varvoglis H., Dvorak R., 2005, Celest. Mech. Dyn. Astron., 92, 71
Vokrouhlický D. et al., 2017, AJ, 153, 270
Vokrouhlický D., 1998, A&A, 335, 1093
Vokrouhlický D., Nesvorný D., 2008, AJ, 136, 280
Vokrouhlický D., Bottke W. F., Chesley S. R., Scheeres D. J., Statler T. S., 2015, in Michel P., DeMeo F. E., Bottke W. F., eds, Asteroids IV. University of Arizona Press, Tuckson, p. 509
Wang X., Hou X., 2017, MNRAS, 471, 243
Wolf M., 1907, Astron. Nachr., 174, 47

Wong I., Brown M. E., 2015, AJ, 150, 174
Čapek D., Vokrouhlický D., 2004, Icarus, 172, 526
Šidlichovský M., Nesvorný D., 1996, Celest. Mech. Dyn. Astron., 65, 137

APPENDIX A: DETERMINATION OF THE JOVIAN TROJAN PROPER ELEMENTS

Here we briefly review our approach to compute synthetic proper elements for the currently known Jovian Trojan population. The method is based on Milani (1993), see also Brož & Rozehnal (2011), though we needed several modifications of the digital filters in order to stabilize determination of the proper elements for Trojans having very small libration amplitude. Our dynamical model included four giant planets, with barycentric corrections to compensate for the indirect perturbations for terrestrial planets. This arrangement suitably speeds up computations when dealing with the whole population of many thousands of Trojans. Nevertheless, we also checked validity of our results using a dynamical model including also the terrestrial planets in a full-fledged manner for a sub-sample of Trojans (notably the low-$\delta V_{\rm P}$ that is of interest here). No significant differences were observed. The initial planetary state vectors were taken from the JPL ephemerides and those of the Trojans from the `AstOrb` catalogue as of 2020 April 28, from which their population was also identified.

We used well-tested numerical package `swift` (e.g. Levison & Duncan 1994), specifically the MVS2 symplectic integrator (e.g. Laskar & Robutel 2001), that we adapted for our application in several ways. The most important was an implementation of digital filters, helping us to eliminate short-period and forced terms from osculating orbital elements, necessary for identification of the proper terms. Due to the absence of the direct perturbations from the terrestrial planets, we can allow a fixed integration time-step of 0.25 yr. The input sampling into the filtering routines was 1 yr. We used a sequence of the convolution (Kaiser-window) filters A A B (e.g. Quinn, Tremaine & Duncan 1991) with decimation factors 10 10 3, which were applied to the non-singular elements $z = k + \imath h = e\,\exp(\imath\varpi)$ and $\zeta = q + \imath p = \sin I\,\exp(\imath\Omega)$. The intermediate time window for this filtering procedure and output time-step was 300 yr. At this stage, the short-period terms with periods comparable to planetary orbital periods or the libration period were efficiently suppressed from the resulting mean values $\bar{z}$ and $\bar{\zeta}$ of eccentricity and inclination variables. We then accumulated batches of 2048 values of $\bar{z}$ and $\bar{\zeta}$, and applied Fourier transformation (in particular the FMFT method from Šidlichovský & Nesvorný 1996), on the output. After rejecting signal associated with forced planetary frequencies (such as g_5, g_6, or s_6 to recall the principal ones), we were left with the proper values $e_{\rm P}$ for the eccentricity and $I_{\rm P}$ for the inclination as the amplitude of the remaining dominant terms. Our simulation spanned the total of 30 Myr, and we computed proper elements in the $\simeq$600 kyr window described above many times over intervals with 100 kyr shift in their origin. This way we had a series of many tens of proper element realizations, allowing to access their stability and compute their mean and variance. We also observed that the series of individual $e_{\rm P}$ and $I_{\rm P}$ still contained long-period signal (periods $>$1 Myr), which in future studies may call for extension of integration windows. At this moment, we however, satisfied ourselves with our set-up. We also used the above outlined procedure for the semimajor axis a, but instead of applying FMFT on its mean values we simply computed its mean value $\bar{a}$ over a 1 Myr interval. This helps us to determine semimajor axis value of the libration centre for a given Trojan orbit.

In order to obtain a reliable information about a stable libration amplitude we need to apply a different method that has been implemented in our code in parallel to computation of $e_{\rm P}$ and $I_{\rm P}$. This is because the corresponding libration frequency is fast, $f \simeq 2.434\,\mathrm{deg\,yr^{-1}}$ and $360^\circ/f \simeq 148$ yr, and must not be under-sampled. A delicate issue consists of the fact that, at the same time, one has to suppress terms with period even shorter than the libration period, namely those which are related to orbital periods of giant planets (principally Jupiter $\simeq$11.86 yr). We thus applied convolution filters B B, with decimation factors 3 3, to the osculating values of the semimajor axis a and the longitude difference $\lambda - \lambda'$ (the orbital elements labelled with prime correspond to Jupiter), a resonant argument of the Trojan tadpole motion. These intermediate (mean) values of a and $\lambda - \lambda'$ are computed with a 9 yr cadence. In the next step, the intermediate $a - a'$ were fitted by a straight line and the constant term a_0 was subtracted. In the same way, the intermediate angle $\phi = \lambda - \lambda' - \chi$, where $\chi = \pm 60^\circ$ depending on the L4 and L5 libration points, was fitted by a straight line and the constant term ϕ_0 was subtracted. Effectively, after subtractions of the mean values was done, the tadpole motion around the Lagrange point centres in these rescaled, zero-averages $a - a'$ versus ϕ coordinates is centred at the origin. Consequently, the polar angle ψ defined as (see e.g. Milani 1993, a and a' in au)

$$\psi = \arctan\left(\frac{a - a'}{0.2783\,\phi}\right) \tag{A1}$$

can be unfolded by 360°, fitted by a straight line, with the slope defining the libration frequency f. The libration amplitudes $da_{\rm P}$ (in au) and D (in deg) are computed by the Fourier transform as amplitudes of spectral terms with frequency f. This second step uses a 1 kyr cadence. Finally, we apply another averaging of $da_{\rm P}$ and D values, defined on a simple running window with the output time-step of 1 Myr. Both $da_{\rm P}$ and D may be considered as the third proper orbital element alongside of $e_{\rm P}$ and $I_{\rm P}$.

We note that the value of libration centre $\bar{a}$ is not universal for all Trojans. Instead, its value functionally depends on the proper elements ($da_{\rm P}$, $e_{\rm P}$, $I_{\rm P}$) or (D, $e_{\rm P}$, $I_{\rm P}$), see Fig. A1. Some authors (e.g. Brož & Rozehnal 2011; Rozehnal et al. 2016) thus define an alternative set of proper elements ($a_{\rm P} = \bar{a} + da_{\rm P}$, $e_{\rm P}$, $I_{\rm P}$).

We determined the above-introduced parameters, including different variants of orbital proper values and their uncertainty, for 7328

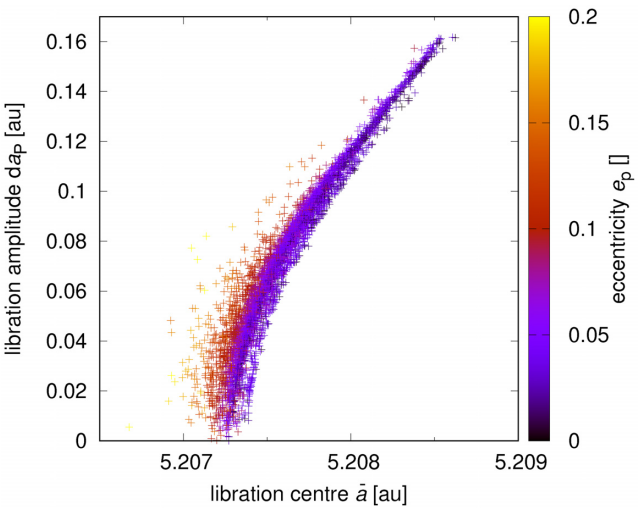

Figure A1. Libration amplitude $da_{\rm P}$ versus libration centre $\bar{a}$ for Trojans in the L4 region. Colour corresponds to the proper eccentricity $e_{\rm P}$. The dependence of $\bar{a}(da_{\rm P}, e_{\rm P})$ is systematic, indicating a functional dependence.

Jovian Trojans, population as of 2020 April. These data can be found on https://sirrah.troja.mff.cuni.cz/~mira/mp/trojans_hildas/.

APPENDIX B: ARE THERE MORE LOW-δV_P COUPLES?

As also suggested by data in Fig. 6, the brief answer to the topic of this Appendix is probably positive, but a full analysis if this issue is left to the future work. Here we only restrict ourselves to illustrate difficulties one would quickly face in attempting to prove the past orbital convergence on a Gyr time-scales for most of the candidates.

Let us consider another low-δV_P candidate couple characterized by small values of proper orbital elements (da_P, e_P, $\sin I_P$), which helps to minimize the unrelated background Trojan population (Section 2). Staying near the L4 libration point, we find 219902 (2002 EG_{134}) and 432271 (2009 SH_{76}) at $\delta V_P \simeq 4.9\,m\,s^{-1}$ distance. This couple has also appreciably small probability $p \simeq 1.5 \times 10^{-6}$ to be a random fluke and it has been highlighted by a green circle in Fig. 6. The proper elements read $da_P \simeq (7.0372 \pm 0.0004) \times 10^{-3}$ au, $e_P \simeq (3.87534 \pm 0.00004) \times 10^{-2}$ and $\sin I_P \simeq (9.496 \pm 0.003) \times 10^{-2}$ for (219902) 2002 EG_{134}, and $da_P \simeq (7.2950 \pm 0.0006) \times 10^{-3}$ au, $e_P \simeq (3.87652 \pm 0.00004) \times 10^{-2}$ and $\sin I_P \simeq (9.469 \pm 0.002) \times 10^{-2}$ for (432271) 2009 SH_{76} (for reference, we again mention their quite small libration amplitudes 1.44°, resp. 1.48°). This is a configuration reminiscent of the (258656) 2002 ES_{76}–2013 CC_{41} case, though each of the three proper elements is slightly larger now. The relative velocity δV_P is again entirely dominated by the proper inclination difference, this time somewhat smaller than in the (258656) 2002 ES_{76}–2013 CC_{41} case (only ≃0.015°). Assuming geometric albedo value 0.075, we obtain sizes of ≃12.8 km and ≃(7.3–8.1) km for (219902) 2002 EG_{134} and (432271) 2009 SH_{76}, considering absolute magnitude values from the major three small-body ephemerides sites as above. While little larger, it still places this couple into the same category of very small Trojans as (258656) 2002 ES_{76}–2013 CC_{41}.

We repeated the convergence experiment using geometrical clones from Section 3.3.1. In particular we considered nominal (best-fitting) orbits of (219902) 2002 EG_{134} and (432271) 2009 SH_{76}, and for each of them we constructed 20 geometrical clone variants of the initial data at MJD58800 epoch. We again used information from the `AstDyS` website and noted that both initial orbits of components in this possible couple have smaller uncertainties in all orbital elements than the orbits of (258656) 2002 ES_{76} and 2013 CC_{41}. This is because their longer observation arcs and more data available for the orbit determination. We propagated these 42 (21+21) test bodies backwards in time to 1.5 Gyr before present. Perturbations from all planets were included and every 500 yr configuration of the nominal orbits and accompanied clones for the two bodies compared. A criterion for convergence included $\delta V \leq 2\,m\,s^{-1}$ from equation (3), and small eccentricity and inclination differences. In particular, we required $\delta e \leq 10^{-4}$ and $\delta I \leq 0.029°$. These values are only slightly larger than the difference in the corresponding proper values and each represent a few metres per second contribution in (1).

Results are shown in Fig. B1 which has the same structure as the Fig. 9, previously given for the (258656) 2002 ES_{76} and 2013 CC_{41} couple. The main take-away message is in the bottom panel, which shows maximum nodal difference between clones of (219902) 2002 EG_{134} and its nominal orbit as a function of time to the past. The slope of the initially linear trend (lasting approximately 50 Myr) is simply given by maximum δs proper frequency among clones from the initial data difference. The non-linearity, which develops at later epochs, is due to orbital long-term chaoticity. While for the (258656) 2002 ES_{76} and 2013 CC_{41} couple the chaotic effects were very minimum, the nodal difference between (258656) 2002 ES_{76} clones and the nominal orbit increased to only ≃4° in 1.5 Gyr. At the end of our run the nodal difference expanded to ≃260°. Given the very limited number of clones we had, this works again identification of convergent solutions. Note that beyond ≃970 Myr, where we would expect more convergent cases, we could satisfy the convergence criteria of only few metres per second described above only rarely. CPU-demanding effort with many more clones would be needed to achieve the desired convergence limits.

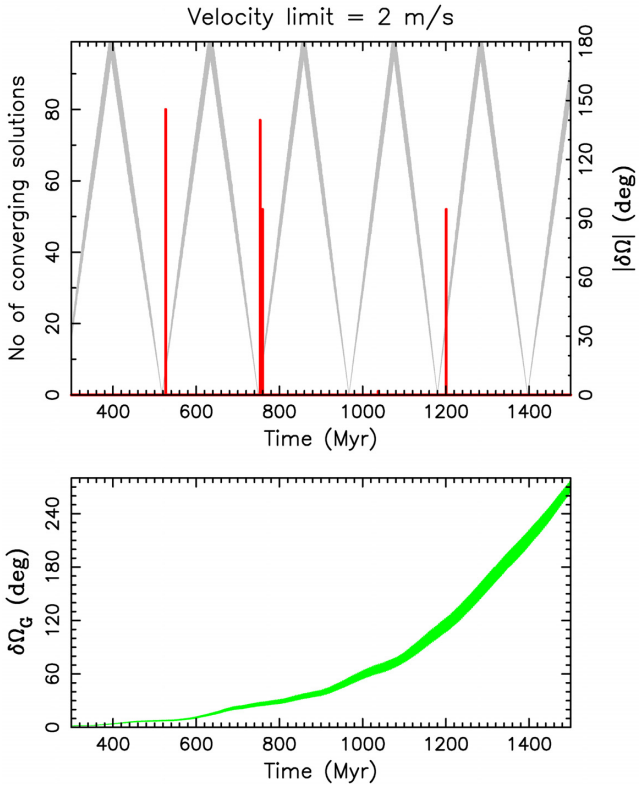

Figure B1. The same as Fig. 9 but for the (219902) 2002 EG_{134}–(432271) 2009 SH_{76} couple of Trojans: past orbital histories of nominal orbits and 20 geometrical clones each compared every 500 yr and convergent solutions within $\delta V \leq 2\,m\,s^{-1}$ limit combined in 50 kyr bins. Top panel gives the number of solutions for all possible combinations of clones (red histogram). The grey line gives $|\delta\Omega|$ of the nominal orbit of (219902) 2002 EG_{134} and (432271) 2009 SH_{76} (see also the right ordinate). The green line at the bottom panel shows the maximum difference in longitude of ascending node between the clones of (219902) 2002 EG_{134} and the longitude of ascending node of its nominal orbit, compared with the same information for (258656) 2002 ES_{76} given in Fig. 9).

We repeated the same experiment for several other candidate couples from the small-δV_P sample, including the case of (215110) 1997 NO_5–2011 PU_{15} (see Fig. 2), but observed even faster onset of the clone diffusion in the Trojan orbital phase space. This was due to their large e_P and/or $\sin I_P$ values, as well as larger libration amplitudes. Their systematic analysis is beyond the scope of this paper.

This paper has been typeset from a TEX/LATEX file prepared by the author.